Distributed Event-Triggered Control for Multi-Agent Systems with Second-Order Dynamics

Mayank Sewlia

Distributed Event-Triggered Control for Multi-Agent Systems with Second-Order Dynamics

Research Thesis

Submitted in partial fulfillment of the requirements
for the degree of Master of Science in Aerospace Engineering

Mayank Sewlia

Submitted to the Senate
of the Technion — Israel Institute of Technology
SIVAN 5780 Haifa June 2020

This research was carried out under the supervision of Prof. Daniel Zelazo, in the Faculty of Aerospace Engineering.

Some results in this thesis have been published as an article by the author and research collaborators in a conference during the course of the author's masters research period, the most up-to-date versions of which being:

[1] M. Sewlia and D. Zelazo, "Distributed event-based control for second-order multi-agent systems," in *2019 27th Mediterranean Conference on Control and Automation (MED)*, pp. 310-315, IEEE, 2019.

Acknowledgements

Foremost, I would like to express my sincere gratitude to my advisor Prof. Daniel Zelazo for his continuous support towards my M.Sc studies and research. His guidance helped me in all the time of research, administrative tasks and writing of this thesis.

Besides my advisor, I would like to thank the rest of my exam committee: Prof. Leonid Mirkin and Prof. Yaakov Oshman, for their time, insightful comments and hard questions.

I also acknowledge the generous financial help of the Technion - Israel Institute of Technology.

Contents

List of Figures

Abstract

The focus of this thesis is to study distributed event-triggered control for multi-agent systems (MAS). In event-triggered control, periodic task execution is replaced with deliberate, opportunistic, and aperiodic task execution, thereby reducing the load on communication and computation resources. We consider mainly two problems in this field, *event-triggered consensus control* and *event-triggered formation control*.

In event-triggered consensus control, we propose state-dependent event triggering conditions to achieve consensus for a team of agents modeled with double-integrator dynamics. We study two event-based consensus algorithms. In the first algorithm we guarantee the agents reach position consensus with a non-zero constant final velocity. The second algorithm guarantees that the agents reach position consensus with a zero final velocity.

In event-triggered formation control, we study bearing-based event triggering conditions to achieve formation stabilization for systems with double-integrator dynamics. First, we design a controller that makes use of local agent state measurements along with the measured bearing states to achieve a stationary final formation. On this newly designed controller, we propose an event-triggered condition (ETC) which drives the sensing and control updates of the agents along with a proof that the inter-event time is strictly positive. Second, we restrict ourselves to only relative states and design an ETC that is edge dependent and drives the control updates of the agents.

All the proposed schemes are distributed in the sense that no global parameter is required and agents locally determine and evaluate trigger conditions. We use Lyapunov theory to provide convergence and stability proofs for the above problems and verify the results using simulation examples.

Abbreviations and Notations

$\mathbb{R}$	:	Set of real numbers
$\mathbb{R}_{\geq 0}$	:	Set of non-negative real numbers
$\mathbb{N}$	:	Set of natural numbers
$\mathcal{G}$	:	A graph
$\mathcal{E}$	:	Set of graph edges
$\mathcal{V}$	:	Set of graph nodes (vertices)
L	:	Graph Laplacian
H	:	Incidence matrix
$\langle \cdot, \cdot \rangle$	:	Real dot product
$\Vert \cdot \Vert$	:	Euclidean norm(2-norm)
$\mathbb{1}_n$	:	n-dimensional vector with all entries 1
I_n	:	n-dimensional identity matrix
$\otimes$	:	Kronecker product
$\inf(\cdot)$	:	Infimum
$\min(\cdot)$	:	Minimum
ZOH	:	Zero Order Hold
ETC	:	Event-Triggered Control

Chapter 1

Introduction

Multi-agent systems (MAS) are systems composed of multiple dynamic units that interact with each other and are characterized by their autonomy, local perspective, adaptability and decentralization. An agent is an entity that takes the shape of the problem it is defined in, such as a human in a population study, an autonomous robot in a multi robot systems, a cell in an organism or an interface agent in a user-computer interaction. The collective behavior of multiple interacting agents come with an advantage of large-scale spatial distribution, ease of deployment, robustness, high scalability and low cost. These systems are recently gaining traction due to their broad application in several fields such as control theory, distributed computation, nanosystems, social networks, power systems, microeconomics theory, operational research and embedded systems. Specifically in control theory, the applications are in formation flying, task allocation problem, optimization and estimation, coverage control, attitude alignment among multiple spacecrafts and sensor management problems [1–5].

In centralized systems, a single entity executes a series of tasks to obtain a desired result, whereas in distributed systems the same goal is accomplished by multiple entities communicating with each other and working in parallel. The need for distributed systems arises because many real world systems are too large and complex and require a multitude of processors, none of which possess entire system knowledge, to obtain desired results. Additionally, there are limitations on the amount of information shared between these agents and it might be impractical to share all available information and convert the problem to a centralized one [6].

Consensus problems, first studied in control theory in [7], is defined as the process to reach an agreement on a quantity of interest that depends on the state of all agents. A consensus protocol is an interaction rule that defines the information exchange between an agent and its neighbors. Consensus protocols provide a direct connection between graph theory and dynamical systems which has come as a handy tool in performing distributed computation over networks [8]. Consensus problems also provide a platform to study how the underlying graph topology directs the evolution of the dynamical system over it. It finds application in problems such as flocking, swarming and rendezvous [2, 9].

Formation control problems, a specialized version of the consensus problem, aims to achieve a target geometric formation shape by defining constraints on the relative states of the agents. These problems are interesting in the sense they exhibit and generate complex behavior and patterns via simple interaction between agents. Such problems are generally characterized by the sensing capabilities of each agent: such as agents equipped with position sensors, displacement sensors, distance sensors and/or bearing measuring sensors. In position-based control, agents sense their own positions to achieve a desired formation and in displacement-based control, agents sense their relative positions with respect to their neighbors. In distance-based control, similar to displacement-based control agents sense their relative positions with respect to their neighbors but in their own local coordinate systems, and finally in bearing-based control, agents sense the relative bearings with respect to their neighbors in a global frame [10, 11]. In bearing-based formation control, the focus of this work, the target formation is specified by inter-agent bearings, the sensing measurements are relative bearing vectors and the agents actively control their accelerations. As seen in [12] and [13], bearing measurements are often cheaper to sense and a formation specified by bearings is invariant to translation and scaling, thereby providing easy maneuverability in these aspects. Most recently, [14] proposed several bearing-only control laws for varied agent models including single-integrator, double-integrator and unicycle dynamics.

In the study of MAS, an assumption of continuous communication between agents and continuous actuator updates is very common. However, in real world implementations on digital beds with wireless communication such assumptions can lead to inefficient utilization of resources or worse, failure to execute said tasks. For example, consider a sensor-actuator system regulating the temperature of a room. Here, the sensor can be asked to obtain new sensing measurements as fast as possible and the actuator can act accordingly. But once the temperature is brought to a desired level, such fast sensing is not required as it is a waste of resource. This can be mitigated by sensing as fast as possible when the situation demands and slow the sensing frequency at other times. In another example, consider the temperature regulation of a mega facility that requires multiple sensors placed at various locations and a single centralized actuation (air-conditioning) mechanism. These sensors communicate wirelessly with each other and agree on a common temperature reading which is then communicated to the actuator. In this scenario, the shared network may be overloaded when all the sensors transmit at the same time resulting in delays, packet losses and overall degradation of system performance. To avoid such situation, the sensors need to sense at certain intervals and communicate with the neighboring sensors only when the need arises. But how do we design such intervals? This question is answered by event-triggered control where we determine an upper bound for worst case execution time by observing the state trajectories of the system [15–17].

1.1 Literature Review

While the field of event-triggered control of multi-agent systems is rapidly growing, our focus is on applying this mechanism to solve problems of communication and actuation between agents to achieve a common goal. The two main areas of focus here are to solve the consensus and formation control problems using event-triggered schemes.

1.1.1 Event-triggered Control

In the existing literature, the assumption of very high sampling frequency and actuation rate is very common. This is difficult to maintain as real world implementations on digital beds have limited communication and processor capabilities [15]. Additionally, once the update rate crosses a certain threshold, there is no improvement in the final convergence accuracy. As a result, we need to find a suitable update frequency while still achieving a desired accuracy. Moreover, this update frequency also depends on the current states of the system and varies throughout the evolution of the agents. Hence, it is intuitive to sample and update states at higher frequencies only when the situation demands, and sample at lower frequencies otherwise. To solve this problem, we make use of event-triggered control (ETC) where we opportunistically and deliberately find sampling and update instants without compromising the final results [18]. In [19], there is an extensive review on the topic of event-triggered control studying the motivation, methodology, challenges and applications of such a control in distributed systems. We use ZOH to generate a piecewise continuous signal from discrete values of control at event-times. ZOH is the most commonly used hold in the event-triggered literature, but there are other types of hold such as system-matched hold studied in [20]. System-matched hold is a generalized hold that matches the system dynamics with the dynamics of the hold. Although higher order holds are seldom used in the event-triggered literature, different types of holding mechanisms can be found in Chapter 5 of [21] and [22].

Chapter 2 provides an extensive review about the field of event-triggered control.

1.1.2 Event-triggered Consensus Control

Event-triggered consensus control, first studied in [15] where a time dependent event based condition is presented for a centralized controller and later extended to a distributed case. Related to this chapter are [23–25]. In particular [23] proposes a time dependent event-triggering function for first and second order dynamics to achieve average velocity consensus. In [24], event-based protocols on single integrator dynamics involving both fixed and switching topology is analyzed. In addition, it provides bounds on the sampling period in terms of eigenvalues of the graph Laplacian. The work [25] investigates the problem of synchronization in complex networks and provides conditions to ensure that infinitely frequent triggering is excluded by providing lower bounds on inter-event times. Furthermore most of the current work on event-based control focuses on time-dependent thresholds instead of state-dependent ones. This approach requires the system to have prior knowledge of the smallest non-zero eigenvalue of the graph laplacian matrix and the event triggered condition (ETC) is updated continuously [26]. This, however, may not be practical when the graph has switching topology or if an agent is disconnected from the system. In [27], the authors study event-triggered consensus control of multi-agent systems with double-integrator dynamics. Here the information graph for position and velocity sharing are heterogeneous and event-triggered conditions for centralized and distributed cases are presented. The authors in [28] study event-triggered consensus problem in the presence of packet losses and communication delays, whereas the authors in [29] study the formation control problem with connectivity constraints. In [27–29], the event-triggered conditions depend on the eigenvalues of the Laplacian matrix and they share an identical structure where the sampling error functions are bounded by an exponential threshold function thereby also requiring synchronized clock data. The discussion in [30] is solely to study event-triggered and self-triggered consensus for MAS with double-integrator dynamics. Here the proposed event-triggered schemes rely heavily on the underlying graph topology, and each agent evaluates multiple triggering functions and violation of any one of these will result in an event. In Chapter 5 of [31], the author studies consensus in a leader-follower network of Euler-Lagrange agents. There are mainly 3 algorithms studied, the first algorithm is built on variable-gain approach, the second algorithm assumes directed graph topology with semi-globally exponential convergence and the third algorithm incorporates gravitational forces. The work in this thesis, on the other hand, aims to avoid any knowledge of parameters depending on the graph topology, such as eigenvalues of the Laplacian matrix, as such parameters are bound to change if the underlying graph changes.

1.1.3 Event-triggered Formation Control

There has been little work in applying event-triggered control to solve formation control problems. Notably, [32] studies bearing-based encirclement formation control using event-triggered schemes for single integrator dynamics. The authors demonstrate global asymptotic stability and prove the avoidance of zeno behavior. However, the event triggering is centralized in the sense that all agents sample and perform control updates at the same instance. The work by [33] provides dynamic event-triggered conditions to solve the formation control problem for agents with linear dynamics. The ETC condition is dynamic in the sense that the event variable 'σ' is gradually reduced closer to 0 from a certain initial value as time progresses. Here, the sensing variables are the states of neighboring agents along with bearing vectors in a global reference frame. Additionally, [34] studies position-dependent event-triggered formation control problem for agents with single integrator dynamics and proposes an algorithm to solve the multitarget selection problem. A generalized gradient based control law is proposed in [35] for agents with single-integrator dynamics and exponential convergence is shown for this controller. Here, the ETC is a function of the smallest eigenvalue of a matrix which is a property of the graph. This is sometimes undesired as it is a global property of the network, and can not cope with communication or agent losses. In Chapter 6 of [31], the author discusses distance-based event-triggered formation control for agents modeled with single-integrator dynamics. The author proposes centralized and distributed event-triggered control laws with the avoidance of zeno-behavior and proves exponential convergence of the distance error system.

1.2 Thesis Contribution

In this section we present a statement of the thesis contributions to event-triggered control of second-order multi-agent systems. This thesis studies and applies event-triggered control strategies to two of the most researched problems in multi-agent systems: consensus and formation control. In consensus, we use these strategies to drive a team of agents to agree on a common value by communicating and sharing information with the neighbors aperiodically. This aperiodic communication is determined by an event-triggering condition which if violated initiates a data transfer between agents. In formation control, we study specifically event-triggered control of bearing-based formation stabilization where the control actions are event driven.

We begin by deriving a state-dependent event-triggered control strategy to solve consensus problems for a continuous time double-integrator dynamics MAS over an undirected network. Firstly, we use Lyapunov theory to arrive at an ETC which solves the average consensus problem. This ETC is used to determine the control updates and communication instants between agents. Secondly, we use this ETC to achieve zero-velocity consensus where the agents agree on a common position with a final zero velocity. This is important when you want to convert a consensus problem to a rendezvous problem. As we will see further in this thesis, converting a consensus problem to a rendezvous problem is done by updating the piecewise continuous controller to a continuous time controller while still operating under the same ETC. Unlike the literature discussed in Section 1.1.2 where agents require some form of global data, all the ETC mechanisms proposed here are distributed i.e., agents locally determine and evaluate trigger conditions. These results are presented in Chapter 3 of this thesis.

We then proceed to solve the bearing-based formation stabilization problem using event-triggered control where we take two approaches in doing this: edge triggering and node triggering. In the first approach, we make use of the bearing-only control law proposed in [14] to arrive at an ETC that is dependent on the relative measurements applied to both agents incident to that edge.[1] Here, the post-trigger response is to

[1] An edge between two agents indicates that a bearing measurement is available.

update the controller when the ETC is violated. In the second approach, we propose a new control law based on the one proposed in [14] to achieve a stationary final formation. Here the ETC is designed over an agent, that along with its self-states uses the collective relative measurement from all its neighbors to evaluate the trigger condition. We further prove that inter-event times are strictly greater than zero. The post-trigger response in this case is to acquire new state measurements and update the controller. All agents are designed with double-integrator dynamics and the proposed control inputs along with the ETC are distributed. These results are presented in Chapter 4.

1.3 Thesis Organization

This work is organized as follows, in Chapter 2, we present an introduction to event-triggered control and review different approaches in designing event-triggered control systems. We then start our main contributions in Chapter 3 where we apply the tools of event-triggered control to the consensus problem. In Chapter 4, we apply these results to the bearing-based formation control problem and in Chapter 5 we conclude the work presented and provide directions for future research. In Appendices we present preliminaries used throughout the thesis, specifically, basic algebraic notions in Appendix A, graph theory is introduced in Appendix B, stability notions of dynamical systeems are introduced in Appendix C and finally, bearing-based formation control is introduced in Appendix D.

Chapter 2

Event-Triggered Control

For a long time, execution of feedback control loops were performed in a periodic manner on digital platforms. With the advent of modern computers, such loop execution in periodic manner has gone out of fashion since modern processors execute multitude of tasks and computation power allotted to each task is limited [17]. This gave rise to aperiodic control or need-base control to address the importance of resource saving in computation, communication and energy. Another motivation as highlighted in [36], comes from implementing hybrid controllers that switch between different algorithms where each algorithms operates at a different frequency. Here the author presents three significant reasons to resort to event-based control. First, it is argued that event-based control is closer to how a human would behave as a controller rather than time-triggered control. Second, event-based control is a natural choice when actuators are on/off in nature, and third, control calculations performed on CPU are performed only when needed thereby saving crucial CPU time usage.

The common approach to designing an event-triggered mechanism is the perturbation approach. The fundamental question asked is how far can the system be perturbed while still guaranteeing some desired behavior? However, we will review various approaches to event-trigger condition design and also classify them based on execution times. In this chapter, we start by classifying common update mechanisms encountered in the literature in the next section.

2.1 Classifications

This section studies types of controller update mechanisms and is built on the results and discussions from [15–17]. These mechanisms are classified into 3 categories: sampled-data control, event-triggered control, and self-triggered control.

2.1.1 Sampled-data Control

Sampled-data control refers to control which takes periodic action irrespective of the current states of the system. Consider the system,

$$\dot{x} = f(x, u),$$

which is stabilized by a controller $u = k(x)$. The controller is designed to update at a constant period, say T seconds. Then,

$$\dot{x} = f(x(t), k(x(t_l))) \quad t \in [t_l, t_{l+1}),$$

for $l \in \mathbb{Z}_{\geq 0}$ and $t_{l+1} - t_l = T$ for all l.

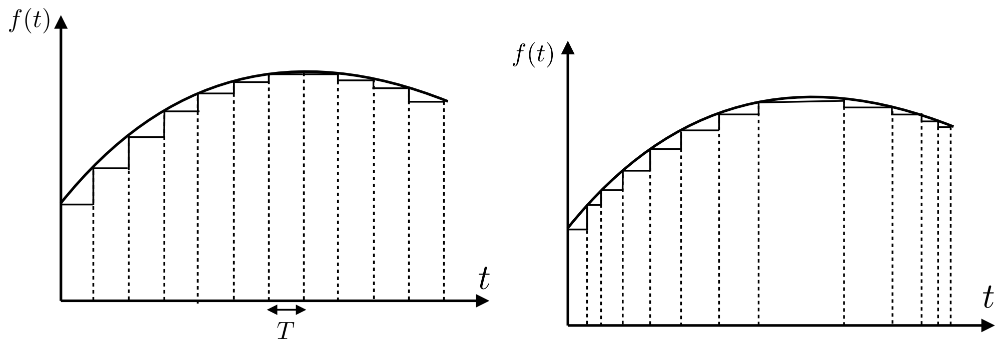

(a) Constant time sampling. (b) Event-triggered sampling.

Figure 2.1: Signal reconstruction using ZOH.

Here the controller is updated at a constant frequency $\frac{1}{T}$ and any hardware designed to work faster than this frequency can be used for implementation. This can be seen in Figure 2.1a where the continuous time signal $f(t)$ is sampled every 'T' seconds and is kept constant between these samples using a zero order hold (ZOH). This sampling frequency is a function of the system and so we naturally ask the question how do we choose such a frequency? For many years the answer was "fast enough" to guarantee a desired final result, however, this notion of "fast enough" keeps changing on the current states of the system. So it makes sense to chose a faster frequency when the situation demands and resort to slower frequency otherwise to save resources, this principle is captured in event-triggered control which is the topic of discussion in the next section.

2.1.2 Event-triggered Control

This section introduces event-triggered control with a basic example from [15]. Event-triggered control, as noted earlier, is reactionary in nature and takes action only when the current state of the system reaches the boundary of a pre-specified region. Unlike sampled-data control, here the sampling time is not constant and keeps varying. This is visualized in Figure 2.1b. The non-uniform event-times are designed based on an event triggering condition and the signal is kept constant between events using a ZOH. Let us illustrate this process with an example. Consider a multi-agent system represented by a graph $\mathcal{G}(\mathcal{V}, \mathcal{E})$ where each agent has the following single-integrator dynamics,

$$\dot{x}_i(t) = u_i(t) \quad i \in \mathcal{V}, \tag{2.1}$$

where $x_i \in \mathbb{R}$ and $u_i \in \mathbb{R}$. The ensemble states of all agents can be written as concatenation of each agent states as follows,

$$\dot{x}(t) = u(t), \tag{2.2}$$

where n is the number of agents. Given L is a Laplacian matrix of the graph $\mathcal{G}(\mathcal{V}, \mathcal{E})$, defined in Appendix B, the ideal controller to achieve consensus for the system in (2.2) is,

$$u(t) = -Lx(t), \tag{2.3}$$

and the closed-loop dynamics of the system as seen in [2] are,

$$\dot{x}(t) = -Lx(t), \tag{2.4}$$

where consensus is defined as follows,

Definition 2.1 ([2]). *Consensus* occurs when a collection of agents agree on a common state value, that is, the dynamics (2.4) asymptotically converges to an agreement set $\mathcal{M} \subseteq \mathbb{R}^n$ defined below,

$$\mathcal{M} = \{x \in \mathbb{R}^n | x_i = x_j, \ \forall \ i, j\}.$$

Now consider the digital implementation of the controller (2.3) and the resulting piecewise continuous controller is,

$$u(t) = -Lx(t_l) \quad t \in [t_l, t_{l+1}),$$

where the interval $[t_l, t_{l+1})$ length is non-uniform for $l \in \mathbb{Z}_{\geq 0}$. Define by

$$e(t) = x(t_l) - x(t), \tag{2.5}$$

which is the measurement error in state, and the resulting closed-loop dynamics are,

$$\dot{x}(t) = -Lx(t_l) = -L(e(t) + x(t)). \tag{2.6}$$

Now our goal is to design event-triggering conditions, such that the system in (2.6) achieves multi-agent consensus. We will use stability theory like 'Lyapunov stability' presented in Appendix C to design such conditions. We chose a candidate Lyapunov function $V(x)$ and examine it along the trajectories of the system and enforce some conditions (ETC) on the error function defined in (2.5) such that $\dot{V}(x)$ is negative semi-definite. Ensuring $\dot{V} \leq 0$, we know $V(x)$ will decrease along the solutions of (2.2) and that these conditions guarantee stability in the sense of Lyapunov. So as long as such conditions are satisfied the control is kept constant using a ZOH and no event is generated, when violated an event is generated and post-trigger response follows.

In this direction, based on the discussion in [15], consider the following Lyapunov function,

$$V(x) = \frac{1}{2}x^T Lx,$$

whose time derivative is,

$$\dot{V}(x) = x^T L\dot{x} = x^T L(-L(e+x)) = -\|Lx\|^2 - x^T LLe.$$

In the above derivative, the first term "$-\|Lx\|^2$" is always non-positive and to ensure $\dot{V} < 0$, we use the submultiplicative property of the spectral norm to arrive at,

$$\dot{V} \leq -\|Lx\|^2 + \|Lx\|\|L\|\|e\|.$$

Now, enforcing the following condition on the error,

$$\|e\| \leq \sigma \frac{\|Lx\|}{\|L\|}, \tag{2.7}$$

for $\sigma \in (0,1)$ we arrive at,

$$\dot{V} \leq (\sigma - 1)\|Lx\|^2$$

which is negative-definite for all $Lx \neq 0$. The condition in (2.7), when met, an event is triggered and the states are sampled and controller updated. The error function "$\|e\|$" is a non-negative and non-decreasing function. The error function rises from 0 until it meets (equals) the threshold function $\sigma\frac{\|Lx\|}{\|L\|}$, at this point, an event is triggered. Then the error function is set to zero and continues to evolve. This can be visualized in Figure 2.2 where the consensus protocol (2.3) is run for 6 agents over a connected and undirected graph. Figure 2.2a shows the states of the agents and Figure 2.2b shows how an event is triggered. As stated earlier, once the condition (2.7) is satisfied, the error function is set to 0 and this process repeats as long as $\sigma\frac{\|Lx\|}{\|L\|}$ is non-zero.

2.1.3 Self-triggered Control

Self-triggered control, first introduced in [37], is proactive in nature and computes the $(i+1)$th sampling time at the ith event time. This is done by making predictions based on the history of states received and knowledge of the system. This process can be illustrated with the following example. Consider a system with general linear dynamics,

$$\dot{x}(t) = Ax(t) + Bu(t), \tag{2.8}$$

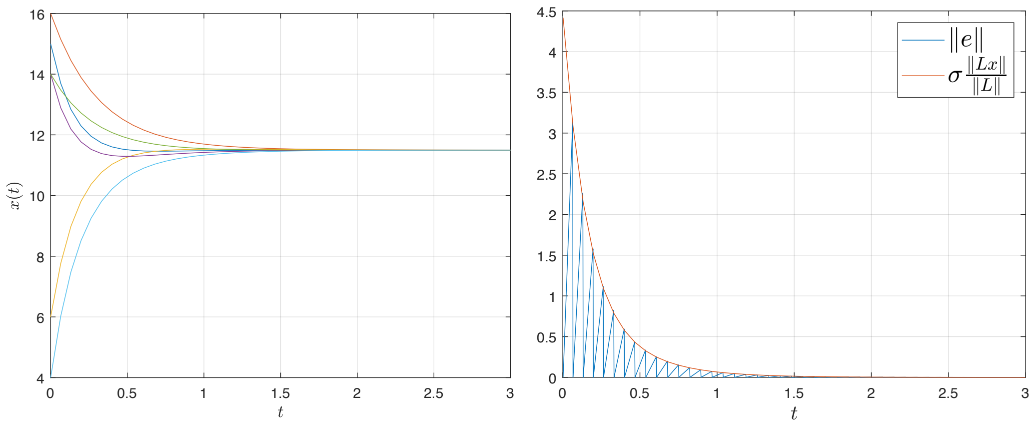

(a) Consensus of 6 agents.

(b) Event-triggering condition.

Figure 2.2: Consensus under the ETC (2.7).

and the ideal linear controller which renders the above system asymptotically stable is,

$$u(t) = Kx(t).$$

The closed-loop dynamics are,

$$\dot{x}(t) = (A + BK)x(t),$$

and following from the discussions in Section 2.1.2, the closed-loop dynamics under the event-triggered scheme are,

$$\dot{x}(t) = Ax(t) + BKx(t_l) = Ax(t) + BK(x(t) + e(t)) = (A + BK)x(t) + BKe(t). \quad (2.9)$$

An ETC can be designed for the system in (2.9) that decides when to sample the states and update the controller. Here however, at triggering time t_l the triggering mechanism evaluates the ETC of the states for $t > t_l$. In the example of linear systems and under the assumption of ideal dynamics, the state trajectory can be given explicitly by,

$$x(t) = \exp\Big((A + BK)(t - t_l)\Big)x(t_l) + \int_{t_l}^{t} \exp\Big((A + BK)(t - t_l)\Big)BKe(\tau)\mathrm{d}\tau,$$

which can be used to determine when the future violation of the error function takes place and the system executes post-trigger actions. This is a simple example of deterministic nature and as real-world irregularities are introduced the analysis gets complicated. However, since the future states are predicted the requirement of continuous sensor measurements is relaxed. Moreover, as shown in [38], the average inter-event times of self-triggered schemes are often lower than that of event-triggered schemes.

To overcome the conservativeness of self-triggered approach and to avoid costly computation resources usage in event-triggered approach, the authors in [39] make the best of both worlds by proposing a scheme in a multi-agent setting that relies on agents making promises to their neighbors about their future states. Consider the task of designing a condition for agent i where the condition is used to decide instants when agent i samples its states to its neighbors. In [39] this is accomplished by having agent i transmit its current state along with its future states to its neighbors and schedules when to transmit/request next update information. This comes from the self-triggered paradigm. Now, if a promise is broken, i.e., states weren't received at the promised times, an event is triggered and new states are immediately demanded which comes from the event-triggered control side.

This thesis focuses on event-triggered control and we proceed in this direction by introducing some approaches commonly encountered in the literature and build upon the tools necessary for the remainder of this thesis.

2.2 Approaches to Event-triggered Control Design

The first approach and most commonly found in the literature is presented in [40]. This approach, commonly called the *discrete-time perturbed linear system* approach is modeled after the perturbation approach to stability analysis presented in [41]. Here, an error in control is introduced and stability analysis follows to bound the deviations of this error. The discussion in Section 2.1.2 is based on this approach and the rest of the work is also modeled after this approach. The results obtained are very conservative and the assumption is that the controller renders the system Input-to-State stable (ISS).

The next approach is performance based design or optimization-based methods. The pioneering work of [42] showed that Lebesgue sampling[1] can outperform periodic control for some quadratic costs in linear plants with Gaussian disturbances. Lebesgue sampling, where the sampling intervals are not canonical, involves forcing the states of a system to a confined region and generating a control signal when the state leaves such said region. This was one of the first works to provide not only a qualitative but a quantitative result on what came to be known, event-triggered sampling mechanisms. In [43], the requirements of full-state feedback is relaxed and partial output-based feedback is used to schedule tasks. Performance is defined by an average quadratic cost and the note guaranteed fewer transmissions compared to traditional optimal periodic executions and additionally, by forgoing 10% of performance the authors obtained 72% of reduction in network usage. The work in [44] characterizes internally stabilizing controllers that guarantee a certain H_∞ performance level and thus the proposed ETC system outperforms optimal time-triggered control except for some atypical cases. By doing this, the authors augment the feedback controllers by enforcing certain performance criterion and stability of the controlled tasks.

[1] Lebesgue sampling refers to a sampling scheme when the system is sampled only when the output has changed by a specified amount.

A large part of recent research is dedicated to reducing conservatism in event-generators and increasing inter-event times while still maintaining stability. This brings us to our next approach in event-trigger design: *dynamic-triggering mechanisms.* Static event generators, for example (2.7), often exhibit zeno-behaviors in the presence of even the slightest disturbances [45], where zeno-behavior is a phenomenon when infinite events are triggered in finite time (see Section 2.3). To circumvent this, dynamic-triggering mechanisms, as presented in [46], introduce an internal dynamic variable that acts as a filter on the threshold function. In contrast to static ETCs, which is analyzed by choosing an appropriate decreasing Lyapunov function $V(t)$, here $V(t)$ need not be a decreasing function rather just upper-bounded by another augmented function $W(t)$ which is a decreasing function. In [45] too, the authors work in the lines of [46], but first they add a minimum inter-event time to each event (time-regularization) to ensure zeno-behavior is avoided and then design a dynamic variable to achieve larger inter-event times.

In [47] the authors take an interesting hybrid-systems approach. Here, as in [45], the authors add a minimum inter-event time h to the mechanism but unlike any previous methods, when an ETC is violated here, the event-generator waits h seconds before taking any action and after the end of the waiting period it continuously takes in new sensor measurements until the ETC is violated again and this process continues. This switching between periodic sampling and continuous event-detection is said to have reduced the workload significantly.

Theoretically, any approach guaranteeing bounds on the states of the system while still maintaining stability can be used to design an event-triggered condition, provided the approach is justified in regards to conservativeness of the regions, ease of implementation on digital beds, complexity of calculations, and so on.

2.3 Zeno-behavior

This section introduces the zeno-phenomenon based on the references [19, 48, 49].
Zenoness[2] describes a phenomenon when a system undergoes an unbounded number of discrete events in a bounded length of time. One common issue in implementing the trigger design is to ensure the exclusion of zeno-behavior, meaning to ensure infinite events are not triggered in finite time.

Denote the sequence of event times by $\{t_l\}_{l\in\mathbb{Z}_{\geq 0}}$. Figure 2.3 captures the essence of zenoness by observing the varied sequences of inter-event times. The sequence of event-times can be characterized into following four categories:

i) **Sampled-data control**: Following our discussion from Section 2.1.1, in a a sampled-data control with constant sampling, as shown in Figure 2.3 be blue

[2]After the Greek philosopher Zeno of Elea who proposed the *Achilles and tortoise* paradox, which said, 'In a race, the quickest runner can never overtake the slowest, since the pursuer must first reach the point whence the pursued started, so that the slower must always hold a lead' [50].

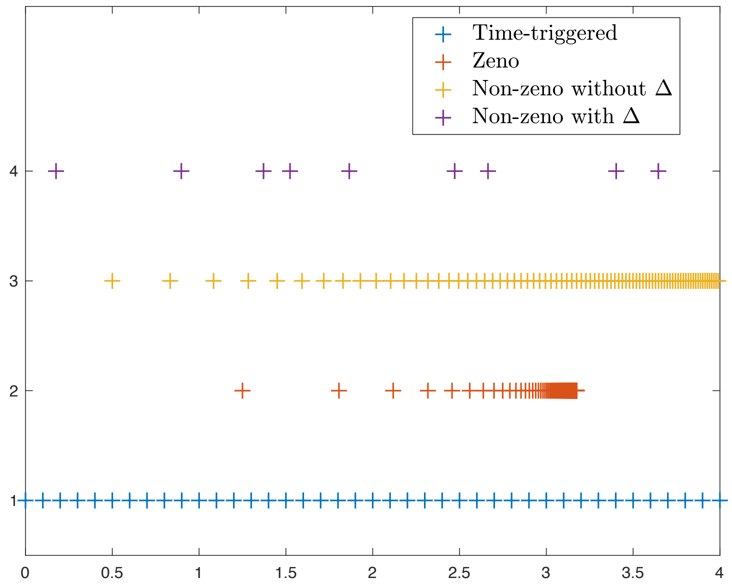

Figure 2.3: Types of sequences of event-times

markers '+', inter-event times are constant irrespective of the current state of the system. For example, consider the following sequence,

$$t_{l+1} - t_l = c,$$

for some $c > 0$ which is the first marker in Figure 2.3. Any controller designed to operate at a frequency higher than the inter-event sampling frequency can be implemented on hardware.

ii) **Zeno behavior**: Consider the marker sequence number two, '+', in Figure 2.3 where the inter-event times are given by,

$$t_{l+1} - t_l = \frac{5}{(l+1)^2},$$

for $l \in \mathbb{Z}_{\geq 0}$. As $l \to \infty$, the event-time $t_l \leq \frac{\pi^2}{3}$, which means there exists an accumulation time before which infinite events will have occured and zeno-behavior is observed. Systems exhibiting such phenomenon cannot be implemented for $t > \frac{\pi^2}{3}$ and hence the need to exclude such behaviors from the trigger design.

iii) **Non-zeno behavior without a minimum inter-event time (Δ)**: In the marker sequence number three in Figure 2.3, '+', the inter-event time is given by,

$$t_{l+1} - t_l = \frac{1}{l+1},$$

for $l \in \mathbb{Z}_{\geq 0}$. As $l \to \infty$, the event-time $t_l \to \infty$, which means theoretically such a controller can be implemented but it needs to act infinitely fast.

iv) **Non-zeno behavior with a minimum inter-event time (Δ)**: The final category is to exclude zeno behavior by finding a *strictly non-zero* lower bound on inter-event times i.e., $\Delta > \epsilon$ where $\epsilon > 0$ and is uniform over all consecutive events. The lower bound must also not be a function of time or the states of the system. This is represented by the fourth marker in Figure 2.3, '+', where the lower bound is $\Delta = 0.1$ which can be implemented by any device operating faster than the frequency of $\frac{1}{\Delta}$. Finding a non-zero lower bound on inter-event time is a stronger condition than avoiding zeno-behavior.

To circumvent the existence of zeno-behavior, periodic event-triggered control has been proposed in the literature [51]. Here, instead of evaluating the trigger condition continuously it is evaluated at a constant period, say 'h'. The next-event time is then given by the following rule,

$$t_{l+1} = \min\{t_l + ih \mid i \in \mathbb{N},\ m(e(t)) > n(x(t_l + ih))\},$$

where the error-term is,

$$e(t) = x(t_l + ih) - x(t_l) \quad t \in [t_l + ih, t_l + (i+1)h),$$

for $i \in \mathbb{N}$. This execution scheme guarantees that the inter-event time is at least h seconds and zeno phenomenon is avoided. Nevertheless, this analysis should be followed by an upper bound on h to ensure the trigger condition is not violated in the interval $[t_l, t_l + h)$ and if violated the system is still guaranteed to remain stable and achieve the said goals.

Chapter 3

Event-triggered Consensus Control

In Chapter 2 we introduced event-triggered controller design and various approaches to stabilize a system. In this chapter we use these tools and apply them to one of the most studied problems in multi-agent systems, the *consensus* protocol. More specifically, we are interested in using these strategies to drive the communication and control of agents. We use Lyapunov-based event-triggering strategy to solve the average consensus problem and the zero-velocity consensus problem.

3.1 Problem Statement

We consider a group of N agents having double integrator dynamics described as,

$$\begin{aligned} \dot{x}_i(t) &= v_i(t), \\ \dot{v}_i(t) &= u_i(t), \end{aligned} \tag{3.1}$$

where $i \in \{1, \ldots, N\}$, $x_i(t) \in \mathbb{R}$, $v_i(t) \in \mathbb{R}$ and $u_i(t) \in \mathbb{R}$ are position, velocity, and control inputs of agent i, respectively. Note that in this study, the states $x(t)$ and $\dot{x}(t)$ are called position and velocity respectively. However, in general, they need not be position and velocity as their definitions can depend on the considered system. Each agent has the ability to sense its states and transmit them to its neighbors over a communication network. Such a network is captured by a static and an undirected graph $\mathcal{G}$ with its corresponding laplacian matrix $L(\mathcal{G})$. A perfect information sharing network is assumed where the transmitted and received states are instantaneously available to the actuators of every agent.

We are interested in distributed control strategies that drive the team of agents to consensus in their states. In this direction, we define two notions of consensus for the multi-agent system comprised of agents with dynamics (3.1).

Definition 3.1. A second order system is said to have achieved *average consensus*, if for all $x_i(0),\ \dot{x}_i(0)\ \in \mathbb{R}$, where $i = 1, 2, \dots, N$,

$$\lim_{t\to\infty}\Big(x_i(t) - \frac{t}{N}\sum_{i=1}^{N} v_i(0)\Big) = \frac{1}{N}\sum_{i=1}^{N} x_i(0) \text{ and}$$
$$\lim_{t\to\infty} v_i(t) = \frac{1}{N}\sum_{i=1}^{N} v_i(0).$$

Definition 3.2. A second order system is said to have achieved *zero velocity consensus*, if for all $x_i(0),\ \dot{x}_i(0)\ \in \mathbb{R}$, where $i = 1, 2, \dots, N$,

$$\lim_{t\to\infty} x_i(t) = c \quad \text{and} \quad \lim_{t\to\infty} v_i(t) = 0,$$

where $c \in \mathbb{R}$ is a scalar constant.

Definition 3.1 states that all agents synchronize their positions and move at a uniform constant velocity which is the average of their initial velocities. Definition 3.2 defines a type of consensus where agents asymptotically agree on a common position with zero velocity i.e., all agents rendezvous to a common point. To achieve the consensus defined in the above definitions, consider the distributed control law proposed in [52] and [53] given by,

$$u_i(t) = -\sum_{j=1}^{n} a_{ij}[(x_i(t) - x_j(t)) + \mu(v_i(t) - v_j(t))], \tag{3.2}$$

where a_{ij} is the $\{i, j\}$ entry of the adjacency matrix $\mathcal{A} \in \mathbb{R}^{n\times n}$ associated with graph $\mathcal{G}$, and μ is a positive scalar. Refer to Appendix B for more information on these matrices.

Denote $x(t) = \begin{bmatrix} x_1 & x_2 & \dots & x_N \end{bmatrix}^T$ and $v(t) = \begin{bmatrix} v_1 & v_2 & \dots & v_N \end{bmatrix}^T$, then the-closed loop dynamics can be written as,

$$\begin{bmatrix} \dot{x}(t) \\ \dot{v}(t) \end{bmatrix} = \Gamma \begin{bmatrix} x \\ v \end{bmatrix}, \quad \text{where} \quad \Gamma = \begin{bmatrix} 0 & I_N \\ -L & -\mu L \end{bmatrix}.$$

The above system reaches *average consensus* for an appropriate choice of gain μ and a connected graph $\mathcal{G}$, as shown in [52, Lemma 4.1].

Now we are ready to design the event-triggered scheme for the proposed problem. The broad gist of an event-triggered scheme is to sample the states $(x_i(t), v_i(t))$ as $(x_i(t_k^i), v_i(t_k^i))$ where the sampled states are constant between the event times $[t_k^i, t_{k+1}^i)$. That is, a zero-order-hold (ZOH) is applied in between the event times. The difference between the last sampled states and the current states of agent i are captured by the following error definitions,

$$\begin{cases} e_x^i(t) &= x_i(t_k^i) - x_i(t), \\ e_v^i(t) &= v_i(t_k^i) - v_i(t). \end{cases} \tag{3.3}$$

Agent i broadcasts its latest states to its neighbors and updates its controller at event times $\{t_0^i, t_1^i, t_2^i, \dots\}$. For notational convenience, we use the notation $(\hat{x}_i, \hat{v}_i)$ for the sampled states $(x_i(t_k^i), v_i(t_k^i))$, and $(x_j(t_{k'}^j), v_j(t_{k'}^j))$ can be equivalently represented as $(\hat{x}_j, \hat{v}_j)$. These event times are determined by the violation of an event triggered condition,

$$f_i(e_x^i(t), e_v^i(t), x_i(t_k^i), v_i(t_k^i)) > 0,$$

for some function $f_i(\cdot)$. Such an event triggered condition, along with driving the actuation and communication between agents must also ensure the stability and thereby convergence of the states of agents to a desired goal. This notion is incorporated in the design of the said condition by using the Lyapunov stability approach to guarantee the trajectories of the agents are bounded and convergent.

In this direction, we would like to consider an event triggered strategy for implementing the second-order consensus control law in (3.2).

Problem 3.1 (Consensus Control) Consider a multi-agent system where the agents' dynamics is described by (3.1). Construct, for each agent $i \in \mathcal{V}$, a state-dependent event triggered condition $f_i(e_x^i(t), e_v^i(t), x_i(t_k^i), v_i(t_k^i)) > 0$, and a distributed control such that the systems achieves,

i) *average consensus* where the communication and control updates are event-driven,

ii) *zero velocity consensus* where the communication between agents is event-driven.

The difficulty here lies in the fact that we aim to design a single event-triggering condition to solve both the problems i.e., we design a single event-triggering condition with different bounds on its parameters to solve two problems: average consensus and zero-velocity consensus. In the former problem, we design an ETC to drive the communication and control updates of the agents and in the latter part, first we design a continuous time controller to solve the zero-velocity consensus problem and then use the ETC from average consensus problem to drive the communication between agents. In the next section we outline the process of obtaining the ETC and present the main results of this chapter.

3.2 Event-triggered Design

In this section, we solve the second order multi-agent system consensus problem with the presentation of an event triggered condition (ETC). The general notion of event based sampling is to define a function that guarantees the error function of a system to always be less than some pre-specified threshold. Such functions generally take the form below,

$$f(\xi, e) \triangleq g(e) - h(\xi), \qquad \xi = \begin{bmatrix} x \\ v \end{bmatrix}, e = \begin{bmatrix} e_x \\ e_v \end{bmatrix}, \tag{3.4}$$

where $g(e)$ is some function of the error and $h(\xi)$ is a threshold that in our case is dependent on the states of the system. The proposed scheme closes the loop every time the error function crosses the pre-specified threshold, i.e., when $f(x,e) = 0$ as defined in (3.4).

The ETC we propose is defined as follows,

$$f_i(e_x^i(t), e_v^i(t), \hat{x}_i(t), \hat{v}_i(t)) = \Big((e_x^i)^2 + \mu(e_v^i)^2\Big) + \Big(\frac{\sigma\alpha_i}{d_i}(-\mu + d_i\alpha_i + \mu d_i\alpha_i)\hat{n}_i^2\Big), \quad (3.5)$$

where e_x^i and e_v^i are sampling errors defined in (3.3), d_i is the number of neighbors of agent i, α_i and σ are positive constants, and $\hat{n}_i$ is the $\{i\}$ element of the vector $\hat{n}(t) = L\hat{v}(t)$. We now use the ETC in (3.5) to achieve *average consensus* and *zero-velocity consensus* as defined in Section 3.1.

3.2.1 Event Triggered Control for Average Consensus

To minimize the controller updates, the controller in (3.2) is modified as,

$$u_i(t) = -\sum_{j=1}^{n} a_{ij}[(x_i(t_k^i) - x_j(t_{k'}^j)) + \mu(v_i(t_k^i) - v_j(t_{k'}^j))], \quad (3.6)$$

for $t \in [t_k^i, t_{k+1}^i)$ and $k'(t) = \arg\min_{l\in\mathbb{N}:t\geq t_l^j}\{t - t_l^j\}$ denotes the last event instant of agent j. The closed-loop dynamics of agent i are,

$$\ddot{x}_i(t) = -\sum_{j=1}^{n} a_{ij}[(x_i(t_k^i) - x_j(t_{k'}^j)) + \mu(v_i(t_k^i) - v_j(t_{k'}^j))].$$

The sequence $\{t_k^i\}_{k\in\mathbb{N}}$ are the time instants when agent i samples its states, while agent j samples its states at $\{t_{k'}^j\}_{k'\in\mathbb{N}}$. This is an asynchronous condition, i.e., agent i can sample its states without receiving/requesting its neighbors to sample their states, and continues to evolve with the last received information from its neighbors. However, agent i will update its controller as soon as it receives any new information from its neighbors. The exchange of information for the system (3.1) with controller (3.6) is shown in Figure 3.1.

In Figure 3.1, the event-triggered condition (ETC) has access to the true state $\{x_i, v_i\}$ of the plant and when the ETC condition is violated, the state is sampled and provided to the controller ($\{\hat{x}_i, \hat{v}_i\}$). These states are available in a sample and hold fashion until the next updated states arrive.

We now provide a result showing that the trigger condition (3.5) with control law (3.6) achieves average consensus for the system.

Theorem 3.1. *Consider the system in* (3.1) *with control* (3.6)*, and assume that the communication graph is connected and undirected. Suppose the event-triggered condition*

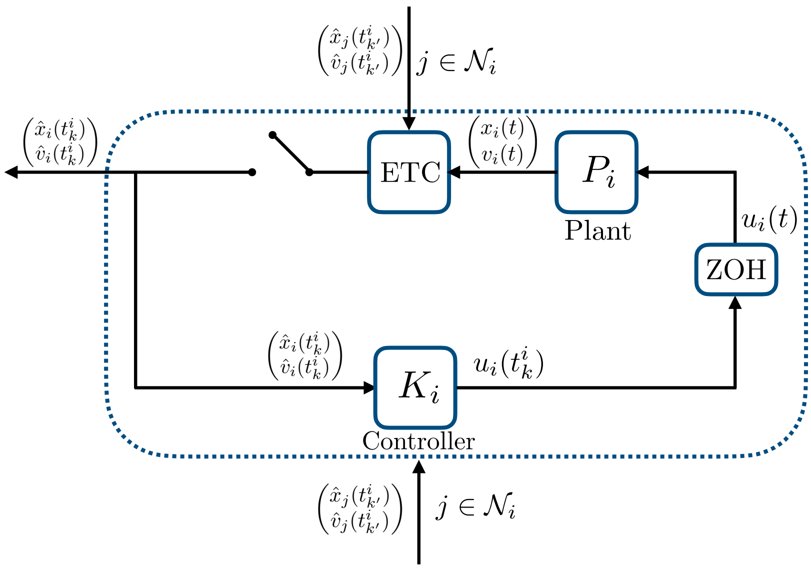

Figure 3.1: Agent i with controller (3.6) and event triggered condition (3.5).

is given by

$$(e_x^i)^2 + \mu(e_v^i)^2 = -\frac{\sigma\alpha_i}{d_i}(-\mu + d_i\alpha_i + \mu d_i\alpha_i)\hat{n}_i^2, \tag{3.7}$$

where e_x^i *and* e_v^i *are sampling errors defined in* (3.3), $\hat{n}_i = \sum_{j\in\mathcal{N}_i}(\hat{v}_i - \hat{v}_j)$, *and* $\mu > 0\ \forall i$. *Then for* $\sigma > 0$,$\epsilon_1 > 0$ *and* $\frac{2\mu+(\sigma-1)\epsilon_1}{2(d_i+\mu d_i)} < \alpha_i < \frac{2\mu-\epsilon_1}{2(d_i+\mu d_i)}$ *and for any initial conditions, the system* (3.1) *with control* (3.6) *achieves* average *consensus.*

Proof. Consider the following candidate Lyapunov function,

$$V(x,v) = \frac{1}{2}x^T L^2 x + \frac{1}{2}v^T L v,$$

where $x \in \mathbb{R}^n$, $v \in \mathbb{R}^n$ and L is a symmetric positive semi-definite Laplacian matrix corresponding to the graph $\mathcal{G}$ as defined in Appendix B. Then the time derivative of $V(x,v)$ can be expressed as,

$$\begin{aligned}\dot{V}(x,v) &= x^T L^2 \dot{x} + v^T L \dot{v},\\ &= x^T L^2 \dot{x} + v^T L(-L\hat{x} - \mu L\hat{v}).\end{aligned}$$

Making use of the error definitions in (3.3), $\hat{x} = e_x + x$ and $\hat{v} = e_v + v$, along with the notation $n = Lv$, we arrive at,

$$\begin{aligned}
\dot{V}(x,v) &= x^T L^2 v - v^T L^2 \hat{x} - \mu v^T L^2 \hat{v},\\
&= x^T L^2 v - v^T L^2 (e_x + x) - \mu v^T L^2 (e_v + v),\\
&= x^T L^2 v - v^T L^2 e_x - v^T L^2 x - \mu v^T L^2 e_v - v^T L^2 v,\\
&= -v^T L^2 v - v^T L^2 e_x - \mu v^T L^2 e_v,\\
&= -\mu n^T n - n^T L(e_x + \mu e_v),\\
&= -\mu n^T n - \sum_i \sum_{j\in\mathcal{N}_i} n_i(e_x^i - e_x^j) - \mu \sum_i \sum_{j\in d_i} n_i(e_v^i - e_v^j)\\
&= -\mu n^T n - \sum_i d_i n_i e_x^i + \sum_i \sum_{j\in\mathcal{N}_i} n_i e_x^j - \mu \sum_i d_i n_i e_v^i + \mu \sum_i \sum_{j\in\mathcal{N}_i} n_i e_v^j.
\end{aligned}$$

Using Young's inequality [54], which states that for a given $x, y \in \mathbb{R}$ and for any $\epsilon \in \mathbb{R}_{>0}$, $|xy| \le \frac{x^2}{2\epsilon} + \frac{\epsilon y^2}{2}$, we can bound $\dot{V}$ as,

$$\begin{aligned}
\dot{V} &\le -\mu \sum_i n_i^2 + \Big(\sum_i \frac{d_i\alpha_i n_i^2}{2} + \sum_i \frac{d_i(e_x^i)^2}{2\alpha_i}\Big) + \Big(\sum_i \frac{d_i\alpha_i n_i^2}{2} + \sum_i \sum_{j\in\mathcal{N}_i} \frac{(e_x^j)^2}{2\alpha_i}\Big) +\\
&\mu\Big(\sum_i \frac{d_i\alpha_i n_i^2}{2} + \sum_i \frac{d_i(e_v^i)^2}{2\alpha_i}\Big) + \mu\Big(\sum_i \frac{d_i\alpha_i n_i^2}{2} + \sum_i \sum_{j\in\mathcal{N}_i} \frac{(e_v^j)^2}{2\alpha_i}\Big)\\
&= \sum_i (-\mu + d_i\alpha_i + \mu d_i\alpha_i) n_i^2 + \sum_i \frac{d_i}{\alpha_i}\Big((e_x^i)^2 + \mu(e_v^i)^2\Big).
\end{aligned}$$

Now we will upper bound the error function, $\frac{d_i}{\alpha_i}\Big((e_x^i)^2 + \mu(e_v^i)^2\Big)$, by another non-negative function $(-\mu + d_i\alpha_i + \mu d_i\alpha_i)\,\hat{n}_i^2$, such that as long as this error function satisfies the bound the derivative of the Lyapunov function can be proved to be negative semi-definite. This condition need not always arise from strictly enforcing the derivative to be negative semi-definite rather can be chosen conveniently as long as the stability proof stands. This idea is explored in [55]. The condition now reads,

$$(e_x^i)^2 + \mu(e_v^i)^2 \le -\frac{\sigma\alpha_i}{d_i}(-\mu + d_i\alpha_i + \mu d_i\alpha_i)\,\hat{n}_i^2 = -\frac{\sigma\alpha_i}{d_i}\beta_i\hat{n}_i^2, \tag{3.8}$$

where $\beta_i = -\mu + d_i\alpha_i + \mu d_i\alpha_i$ and $e_{n_i} = \hat{n}_i - n_i$, arriving at,

$$\begin{aligned}
\dot{V} &\le \sum_i \beta_i n_i^2 - \sum_i \sigma\beta_i\hat{n}_i^2 = \sum_i \beta_i(\hat{n}_i - e_{n_i})^2 - \sum_i \sigma\beta_i\hat{n}_i^2,\\
&= \sum_i \beta_i(1-\sigma)\hat{n}_i^2 + \sum_i \beta_i e_{n_i}^2 - \sum_i 2\beta_i\hat{n}_i e_{n_i},\\
&\le \sum_i \beta_i(1-\sigma)\hat{n}_i^2 + \sum_i \beta_i e_{n_i}^2 + \sum_i \Big(\frac{4\beta_i^2\hat{n}_i^2}{2\epsilon_1} + \frac{\epsilon_1 e_{n_i}^2}{2}\Big),\\
&= \sum_i \Big(\beta_i(1-\sigma) + \frac{2\beta_i^2}{\epsilon_1}\Big)\hat{n}_i^2 + \sum_i (\beta_i + \frac{\epsilon_1}{2})e_{n_i}^2,
\end{aligned} \tag{3.9}$$

is negative semi-definite $\forall$ $\{x, v\}$ given $\sigma > 0$, $\epsilon_1 > 0$ and $(\sigma - 1)\epsilon_1 < 2\beta_i < -\epsilon_1$ which translates to bounds on α_i as $\frac{2\mu+(\sigma-1)\epsilon_1}{2(d_i+\mu d_i)} < \alpha_i < \frac{2\mu-\epsilon_1}{2(d_i+\mu d_i)}$. With the above Lyapunov function, we now can define the compact set $\Omega = \{(x, v) \,|\, V(x, v) \leq c\}$ and let $S = \{(x, v) \in \Omega | \dot{V}(x, v) = 0\}$. Note that $\dot{V} \equiv 0$ in (3.9) is possible only when $\hat{n}_i = 0$ and $e_{n_i} = 0 \implies \hat{n}_i = n_i$ meaning that the velocities are in agreement (i.e., $v \in \text{span}\{\mathbb{1}\}$). We now show that S cannot contain any trajectories where $Lx \neq 0$. To prove this by contradiction, let there be an agent $k \in \mathcal{N}_i$ such that $x_k > x_i$ which ensures $Lx \neq 0$. Then

$$\dot{v}_i = -\sum_{j=1}^{n} a_{ij}[(\hat{x}_i - \hat{x}_j) + \mu(\hat{v}_i - \hat{v}_j)] = -\sum_{j=1}^{n} a_{ij}(\hat{x}_i - \hat{x}_j) > -a_{ik}(\hat{x}_i - \hat{x}_k) > 0,$$

due to our assumption that $x_k > x_i$, which is a contradiction because any trajectory in S must have $\dot{v}_i = 0$. Therefore, S must be of the form $S = \{(x, v) \in \Omega \cap (\text{span}\{\mathbb{1}\}, \text{span}\{\mathbb{1}\})\}$. Invoking LaSalle's invariance principle [41], we conclude that all trajectories starting in Ω must converge to S as $t \to \infty$. ■

When the error grows and the condition in (3.8) is violated, an event is triggered, i.e., when,

$$(e_x^i)^2 + \mu(e_v^i)^2 = -\frac{\sigma\alpha_i}{d_i}(-\mu + d_i\alpha_i + \mu d_i\alpha_i)\hat{n}_i^2.$$

At this instant, $x_i(t) = x_i(t_k^i)$ and $v_i(t) = v_i(t_k^i)$ thus resetting the error function to 0. This process of error function evolving from 0 to a positive value continues until consensus is achieved. Notice that even though the vector $n(t)$ is a function of continuous time 't', the neighbors provide agent i only with the sampled states $\{x_j(t_l^j), v_j(t_l^j)\}_{l\in\mathbb{N}}$ and we can either set the ETC to receive $x_i(t)$ or $x_i(t_k^i)$ without undermining the results. This is explored in the sequel.

We now take a moment to talk about the error dynamics as defined in (3.7). In vector form we can re-write (3.7) as,

$$E_x + \mu E_v = \beta \ \text{diag}(\hat{n}_1^2, \hat{n}_2^2, \ldots, \hat{n}_N^2),$$

where $E_x = \begin{bmatrix}(e_x^1)^2 & \ldots & (e_x^N)^2\end{bmatrix}^T$, $E_v = \begin{bmatrix}(e_v^1)^2 & \ldots & (e_v^N)^2\end{bmatrix}^T$, and $\beta = \text{diag}(\beta_1, \ldots, \beta_N)$ with $\beta_i = -\frac{\sigma\alpha_i}{d_i}(-\mu + d_i\alpha_i + \mu d_i\alpha_i)$. Then when consensus is achieved, $v = c\mathbb{1}$ with c being a constant hence $n_i = 0$ for $i \in \mathcal{V}$. We obtain $E_x + \mu E_v = \beta \ \text{diag}(\hat{n}_1^2, \hat{n}_2^2, \ldots, \hat{n}_N^2) = 0$. As the error function is always non-negative, we have $E_x + \mu E_v = 0$. Concluding that when consensus is achieved the error function goes to 0.

Reducing the communication load in a network comes at a cost of a slower convergence rate. To prove this, define the convergence rate of $V(x, v)$ as [56],

$$\rho \coloneqq \frac{1}{2} \inf \Big\{ -\frac{\dot{V}(x, v)}{V(x, v)} : (x, v) \in S \Big\}.$$

Let ρ_e be the convergence rate with event-based sampling and ρ_w without event-based sampling and our goal is to show $\rho_e < \rho_w$. Then,

$$\rho_e = \frac{1}{2}\inf\Big\{\frac{\sum_i\Big(-\beta_i(1-\sigma)-\frac{2\beta_i^2}{\epsilon_1}\Big)n_i^2}{\frac{1}{2}x^TL^2x+\frac{1}{2}v^TLv}, (x,v)\in S/\mathbf{0}\Big\}, \tag{3.10}$$

and,

$$\rho_w = \frac{1}{2}\inf\Big\{\frac{\mu v^TL^2v}{\frac{1}{2}x^TL^2x+\frac{1}{2}v^TLv}, (x,v)\in S/\mathbf{0}\Big\}, \tag{3.11}$$

and from the conclusion of Theorem 3.1 we infer that $0 < \sum_i(1-\sigma)(\mu - d_i\alpha_i - \mu d_i\alpha_i) - \frac{2\beta_i^2}{\epsilon_1} < \sum_i(1-\sigma)(\mu - d_i\alpha_i - \mu d_i\alpha_i)$ and it can be shown that $\sum_i n_i^2 = v^TL^2v$. Therefore, $\rho_e < (1-\sigma)\rho_w$ implying $\rho_e < \rho_w$.

3.2.2 Event Triggered Control for Zero Velocity Consensus

To achieve zero velocity consensus, we propose a modification to the controller proposed in (3.6). In this case, we provide both the ETC and the controller access to continuous time self-states $\{x_i(t), v_i(t)\}$, which renders the controller to be continuous as opposed to that presented in Section 3.2.1 which is piecewise continuous. This can be noticed in Figure 3.2, which in contrast to Figure 3.1 provides continuous self-states to the controller. The control law is now defined as,

$$u_i(t) = -\sum_{j=1}^{n} a_{ij}[(x_i(t) - x_j(t^j_{k'})) + \mu(v_i(t) - v_j(t^j_{k'}))], \tag{3.12}$$

where $\{x_j(t^j_{k'}), v_j(t^j_{k'})\}$ are the last received states from the neighboring agent j and the closed-loop dynamics are,

$$\ddot{x}_i(t) = -\sum_{j=1}^{n} a_{ij}[(x_i(t) - x_j(t^j_{k'})) + \mu(v_i(t) - v_j(t^j_{k'}))]. \tag{3.13}$$

The control in (3.12) can be represented in vector form as,

$$u(t) = -(\Delta(\mathcal{G})x(t) - \mathcal{A}(\mathcal{G})x(t^j_{k'})) - \mu(\Delta(\mathcal{G})v(t) - \mathcal{A}(\mathcal{G})v(t^j_{k'})),$$

where $\Delta(\mathcal{G})$ and $\mathcal{A}(\mathcal{G})$ are the degree and adjacency matrices of the graph $\mathcal{G}$ defined in Appendix B. The following theorem shows that ETC (3.7) indeed achieves consensus for the system (3.13).

Theorem 3.2. *Consider the system in* (3.1) *with control* (3.12)*, and assume that the communication graph is connected and undirected. Suppose the event-triggered condition is given by* (3.7)*, then for* $\epsilon_2 > 0$*,* $\beta_i > \frac{2\gamma_i(\epsilon_2+2\gamma_i)}{\sigma\epsilon_2}$ *and* $\gamma_i < -\epsilon_2/2$ *and for any initial conditions, the system achieves consensus.*

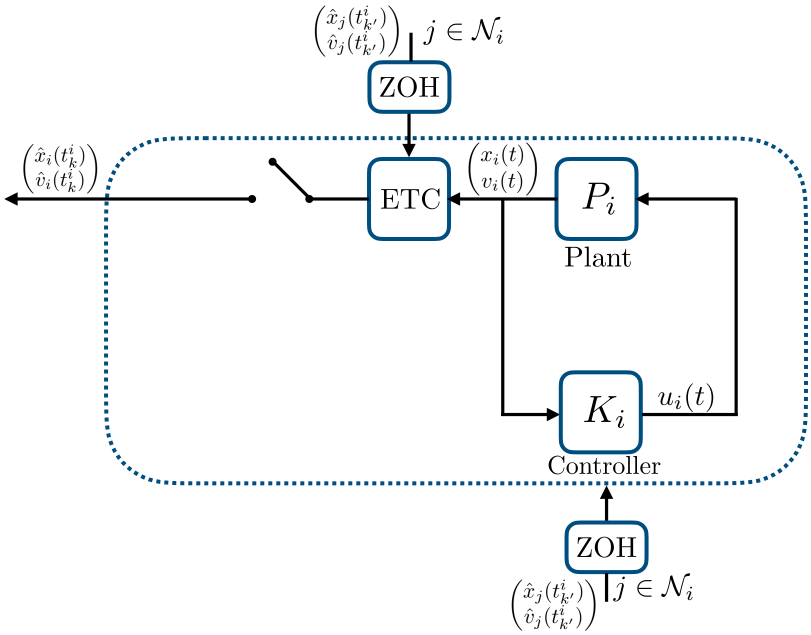

Figure 3.2: Agent i with controller (3.12) and event triggered condition (3.5).

Proof. Consider the following candidate Lyapunov function,

$$V(x, v) = \frac{1}{2}x^T L^2 x + \frac{1}{2}v^T Lv,$$

where L is a symmetric positive semi-definite Laplacian matrix corresponding to the graph $\mathcal{G}$. Then we have,

$$\begin{aligned}\dot{V}(x, v) &= x^T L^2 \dot{x} + v^T L\dot{v},\\ &= x^T L^2 v + v^T L[-(\Delta x - \mathcal{A}\hat{x}) - \mu(\Delta v - \mathcal{A}\hat{v})],\\ &= -\mu v^T L^2 v + v^T L\mathcal{A}e_x + \mu v^T L\mathcal{A}e_v,\\ &= -\mu\sum_i n_i^2 + \sum_i n_i \sum_{j\in\mathcal{N}_i} e_x^j + \mu\sum_i n_i \sum_{j\in\mathcal{N}_i} e_v^j.\end{aligned}$$

Using Young's inequality to bound the above equation and using the condition (3.7), we arrive at,

$$\begin{aligned}\dot{V}(x, v) \le \sum_i \Big(-\mu + \frac{\mu d_i\alpha_i}{2} + \frac{\alpha d_i}{2}\Big)n_i^2 - \sum_i \frac{\sigma}{2}\beta_i\hat{n}_i^2 = \sum_i \gamma_i n_i^2 - \sum_i \frac{\sigma}{2}\beta_i\hat{n}_i^2,\\ = \sum_i \gamma_i(\hat{n}_i - e_{n_i})^2 - \sum_i \frac{\sigma}{2}\beta_i\hat{n}_i^2 \le \Big(\gamma_i - \frac{\sigma\beta_i}{2} + \frac{4\gamma_i^2}{2\epsilon_2}\Big)\hat{n}_i^2 + \Big(\gamma_i + \frac{\epsilon_2}{2}\Big)e_{n_i}^2\end{aligned}$$

which is negative semi-definite for $\epsilon_2 > 0$, $\beta_i > \frac{2\gamma_i(\epsilon_2+2\gamma_i)}{\sigma\epsilon_2}$ and $\gamma_i < -\epsilon_2/2$. We have $\dot{V} \equiv 0$ if and only if $n_i = 0$ which is possible only when the velocities are in agreement (i.e., $v \in \text{span}\{\mathbb{1}\}$), hence using LaSalle's invariance principle [41] and the similar arguments posed at the end of Theorem 3.1, we can conclude that consensus is achieved i.e., $|x_i - x_j| \to 0$ and $|v_i - v_j| \to 0$ as $t \to \infty$. ■

Using the preceding theorem, we would like to determine that the consensus achieved is indeed zero-velocity consensus. In this direction, consider the control in (3.12) and denote,

$$\xi_i = [x_i \ v_i]^T \quad \text{and} \quad \hat{\xi}_i = [\hat{x}_i \ \hat{v}_i]^T,$$

leading to

$$\dot{\xi}_i = C\xi_i - BK \sum_{j \in d_i} a_{ij}(\xi_i - \hat{\xi}_j) - BF \sum_{j \in d_i} a_{ij}(\xi_i - \hat{\xi}_j), \tag{3.14}$$

where $C = \begin{bmatrix} 0 & 1 \\ 0 & 0 \end{bmatrix}$, $B = \begin{bmatrix} 0 \\ 1 \end{bmatrix}$, $K = \begin{bmatrix} 0 & \mu \end{bmatrix}$ and $F = \begin{bmatrix} 1 & 0 \end{bmatrix}$. Then in state space form, the system can be represented as,

$$\dot{\xi}(t) = \Xi_{\mathcal{G}} \ \xi(t) + \Theta_{\mathcal{G}} \ \hat{\xi}(t), \tag{3.15}$$

where

$$\Xi_{\mathcal{G}} = I_N \otimes C - \Delta \otimes B(K + F), \ \Theta_{\mathcal{G}} = \mathcal{A} \otimes B(K + F).$$

Lemma 3.3. *The matrix* $\Xi_{\mathcal{G}}$ *is Hurwitz and* $\exp(\Xi_{\mathcal{G}} t) \to 0$ *as* $t \to \infty$.

Proof. Denoting the eigenvalues of $\Xi_{\mathcal{G}}$ as $\lambda_1 \le \lambda_2 \le \cdots \le \lambda_{2N}$ and expressing the matrix $\Xi_{\mathcal{G}}$ as,

$$\begin{aligned} \Xi_{\mathcal{G}} &= I_N \otimes C - \text{diag}\{d_1, d_2, \ldots, d_N\} \otimes (BK + BF) \\ &= \text{diag}\{C - d_1 BK - d_1 BF, C - d_2 BK - d_2 BF, \ldots, C - d_N BK - d_N BF\}. \end{aligned}$$

The above matrix $\Xi_{\mathcal{G}}$ is a block diagonal matrix and we can study its individual blocks to gain more perspective on its spectral properties. In particular,

$$\det(C - d_i BK - d_i BF) = \det\left(\begin{bmatrix} 0 & 1 \\ -d_i & -\mu d_i \end{bmatrix}\right) = d_i \neq 0,$$

which shows that $\text{rank}(C - d_i BK - d_i BF) = 2$. It follows that,

$$\text{rank}(\Xi_{\mathcal{G}}) = \sum_{i=1}^{N} \text{rank}(C - d_i BK - d_i BF) = 2N,$$

hence the matrix $\Xi_{\mathcal{G}}$ is full rank and consists of only non-zero eigenvalues. The characteristic equation corresponding to the matrix $(C - d_i BK - d_i BF)$ for $i = 1, \ldots, N$ is,

$$f(s) = \begin{vmatrix} -s & 1 \\ -d_i & -\mu d_i - s \end{vmatrix} = s^2 + (\mu d_i)s + d_i,$$

and the roots of the above polynomial are,

$$s = \frac{-\mu d_i \pm \sqrt{\mu^2 d_i^2 - 4d_i}}{2},$$

$\forall \mu, d_i > 0$, the matrices $C - d_i BK - C_i BF$ for $i = 1, 2, \ldots, N$ are Hurwitz stable, implying the matrix $\Xi_{\mathcal{G}}$ is Hurwitz. Since $\Xi_{\mathcal{G}}$ is Hurwitz, $\exp(\Xi_{\mathcal{G}} t) \to 0$ as $t \to \infty$. ■

Theorem 3.3. *Consider a connected and undirected graph $\mathcal{G}$, then under the event triggered condition* (3.7) *control in* (3.12) *achieves zero velocity consensus.*

Proof. From Theorem 3.2 we know that the system achieves consensus i.e., $x_i(t) \to x_j(t)$ and $v_i(t) \to v_j(t)$. Now to prove that this is a zero-velocity consensus, consider the general solution to the state space equation in (3.15) as,

$$\begin{aligned}
\xi(t) &= \exp(\Xi_{\mathcal{G}} t)\xi(0) + \exp(\Xi_{\mathcal{G}} t) \int_0^t \exp(-\Xi_{\mathcal{G}} \tau)\Theta_{\mathcal{G}} \hat{\xi}(\tau) d\tau \\
&= \exp(\Xi_{\mathcal{G}} t)\xi(0) + \exp(\Xi_{\mathcal{G}} t)\Big(-\exp(-\Xi_{\mathcal{G}} \tau)\Xi_{\mathcal{G}}^{-1}\Theta_{\mathcal{G}} \hat{\xi}(\tau)\Big|_0^t \\
&- \int_0^t \exp(-\Xi_{\mathcal{G}} \tau)(-\Xi_{\mathcal{G}})^{-1}\Theta_{\mathcal{G}} \dot{\hat{\xi}}(\tau) d\tau\Big) \\
&= \exp(\Xi_{\mathcal{G}} t)\xi(0) - \Xi_{\mathcal{G}}^{-1}\Theta_{\mathcal{G}} \hat{\xi}(t) + \exp(\Xi_{\mathcal{G}} t)\Xi_{\mathcal{G}}^{-1}\Theta_{\mathcal{G}} \hat{\xi}(0) \\
&+ \exp(\Xi_{\mathcal{G}} t) \int_0^t \exp(-\Xi_{\mathcal{G}} \tau)\Xi_{\mathcal{G}}^{-1}\Theta_{\mathcal{G}} \dot{\hat{\xi}}(\tau) d\tau.
\end{aligned}$$

For a very large t, since $\Xi_{\mathcal{G}}$ is Hurwitz, $\exp(\Xi_{\mathcal{G}} t) \to 0$ as $t \to \infty$ and since consensus is achieved, $\dot{\hat{v}} \to 0$ and the above equation reduces to,

$$\lim_{t\to\infty} \xi(t) = \lim_{t\to\infty} -\Xi_{\mathcal{G}}^{-1}\Theta_{\mathcal{G}} \hat{\xi}(t). \tag{3.16}$$

The matrix $\Xi_{\mathcal{G}}$ is a block diagonal matrix with blocks

$$\begin{bmatrix} 0 & 1 \\ -d_i & -\mu d_i \end{bmatrix},$$

as shown in Lemma 3.3. We see that it's inverse is also a block diagonal matrix with blocks

$$\begin{bmatrix} -\mu & -1/d_i \\ 1 & 0 \end{bmatrix}.$$

The matrix $\Theta_{\mathcal{G}}$ is also composed of blocks with components $\begin{bmatrix} 0 & 0 \\ \times & \times \end{bmatrix}$ and the product of $\Xi_{\mathcal{G}}^{-1}$ and $\Theta_{\mathcal{G}}$ will be matrices with blocks of $\begin{bmatrix} \times & \times \\ 0 & 0 \end{bmatrix}$. Hence, we see that all the even numbered rows of (3.16) which correspond to the velocities of the agents are 0 as $t \to \infty$. Therefore $\lim_{t\to\infty} v_i(t) = 0$ and it follows that $\lim_{t\to\infty} x_i(t) = \text{constant}$. ■

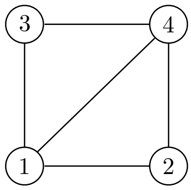

Figure 3.3: Communication graph $\mathcal{G}$ of the multi-agent system.

The conclusion about convergence rate for zero-velocity consensus problem is in lines with that presented at the end of Section 3.2.1 and we conclude that convergence with event-triggered control is slower than without it.

3.3 Simulation results

In this section, we illustrate the theoretical results through simulations for a network of 4 agents with communication graph $\mathcal{G}$ and Laplacian matrix

$$L = \begin{bmatrix} 3 & -1 & -1 & -1 \\ -1 & 2 & 0 & -1 \\ 1 & 0 & 2 & -1 \\ -1 & -1 & -1 & 3 \end{bmatrix},$$

as seen in Figure 3.3. The constants chosen are $\mu = 2,\ \alpha_1 = \alpha_2 = \alpha_3 = \alpha_4 = 0.1$ and $\sigma = 0.9$. If σ is chosen closer to 1 will result in fewer triggers but slower convergence and σ value closer to 0 will result in higher number of triggers with faster convergence.

3.3.1 Average consensus

Figure 3.4 simulates the average consensus case for 4 agents communicating over a network shown in Figure 3.3. The results in Figure 3.4 are consistent with Theorem 1 as all the agents asymptotically reach position consensus with constant final velocity. Since the control law is piecewise continuous, this event based scheme makes use of lesser computing power compared to traditional periodic sampling. The evolution of error and trigger functions for agent 1 is shown in Figure 3.5a. As discussed earlier, the error function increases from 0 in the positive direction until equality is attained in (3.8) and subsequently the error function is reset to zero and this process repeats until consensus is achieved. The threshold function, as indicated in Figure 3.5a is re-evaluated any time new information is received from the neighbors. Figure 3.5b shows the evolution of the Lyapunov function as defined in Theorem 3.1 and we note that $V(x, v) \to 0$ as consensus is achieved.

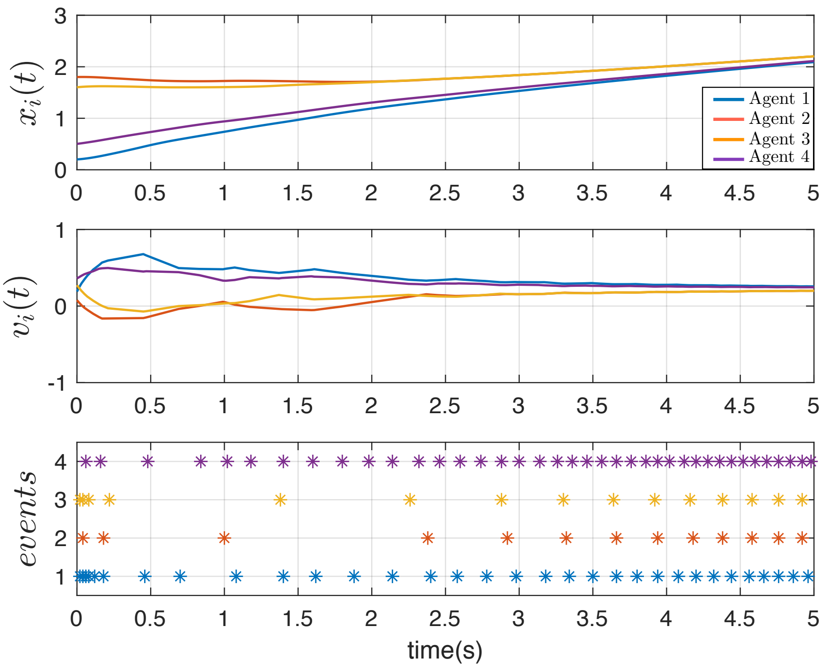

Figure 3.4: Average consensus results showing position and velocity convergence along with instants when an event is triggered.

3.3.2 Zero velocity consensus

The simulation results for agents with closed-loop dynamics (3.13) are shown in Figure 3.6a where we conclude that velocities of all agents converges to zero and positions converge to a constant value consistent with the results of Theorem 3.3. The continuous time controller inputs to individual agents as defined in equation (3.12) is shown in Figure 3.6b and $u_i \to 0$ as the states converge.

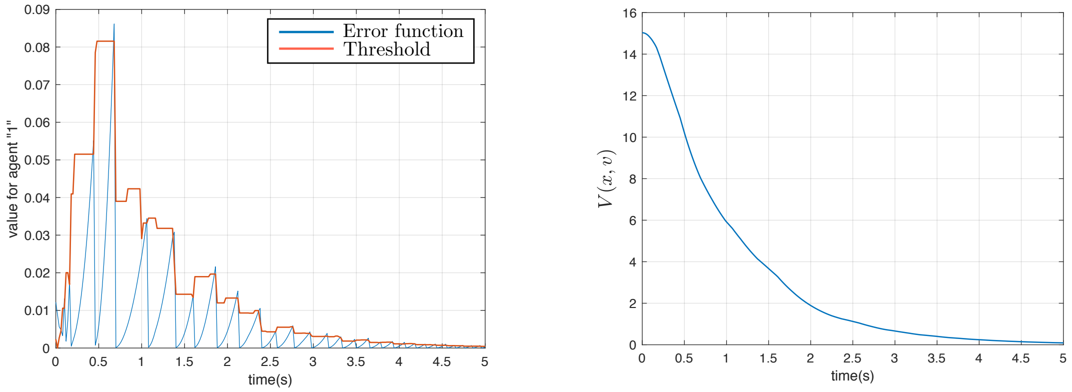

(a) Agent 1 - Error and trigger function.

(b) Evolution of the Lyapunov function.

Figure 3.5: Results pertaining to the average consensus problem.

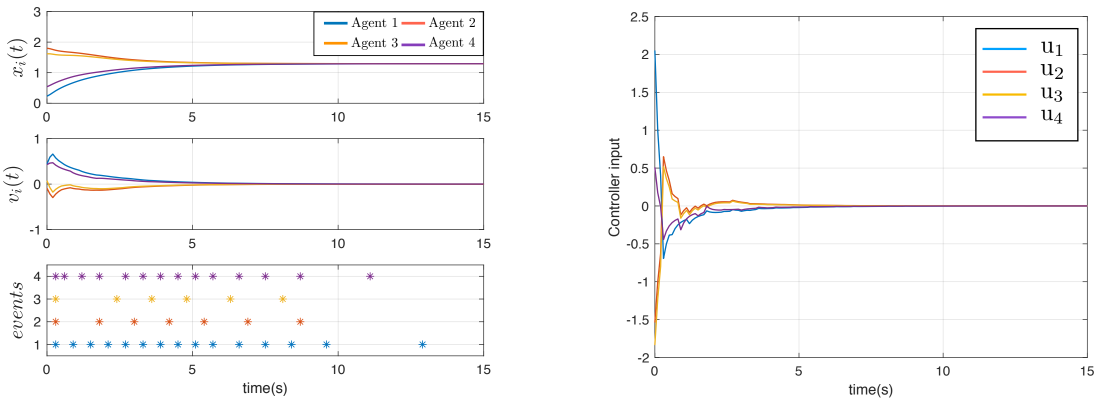

(a) Zero-velocity consensus results showing position and velocity convergence along with instants when an event is triggered.

(b) Controller inputs of all agents.

Figure 3.6: Results pertaining to zero-velocity consensus problem.

Chapter 4

Event-triggered Formation Control

This chapter studies event-triggered bearing-based formation control problems for agents with double-integrator dynamics. Our goal is to derive event-triggered conditions which drive the control and/or sensing updates of the agents. In this chapter we start by presenting a novel controller that solves the bearing-based formation problem. Then we design event-update schemes to solve the bearing-only and bearing-based formation problems.

4.1 Bearing-only Formation Control

In formation control problems, the aim is to drive an ensemble of agents to a desired geometric pattern determined by constraints on their states. These constraints can be specified using relative states between the agents, as is the case in bearing-based formation control. Here, the constraints are defined in the form of inter-agent bearings and the formation is achieved when the measured bearing vector g_{ij}, expressed in a global coordinate frame, arrives at a desired bearing vector $g_{ij}^{\star}$. Bearing only formation control, studied excessively here, defines the desired geometric pattern using bearing measurements. Bearings are d-dimensional vector quantities with unit magnitude that defines the orientation of two connected agents in a global coordinate frame. For more information we refer the reader to Appendix D where we present an introduction to bearing-only formation control and some results from [14].

In this work, we consider multi-agent systems having double integrator dynamics described as,

$$\dot{p}_i(t) = v_i(t),\ \dot{v}_i(t) = u_i(t) \quad i = 1, \ldots, n, \tag{4.1}$$

where $p_i(t) \in \mathbb{R}^d$, $v_i(t) \in \mathbb{R}^d$ and $u_i(t) \in \mathbb{R}^d$ are position, velocity and control inputs of agent i, respectively. While working with double integrator models, it is not sufficient to only sense the relative bearing vectors, as we also need some information on the relative velocities of the agents. This information, in some part, is provided by sensing the rate of bearings $\{\dot{g}_{ij}\}_{(i,j)\in\mathcal{E}}$. Although the velocities of agents need not synchronize, the rate of bearings do i.e., $\{\dot{g}_{ij}\}_{j\in\mathcal{N}_i} \to 0$ as $t \to \infty$. Consider the bearing-only control law presented in [14] for the system defined in (4.1) as,

$$u_i(t) = k_p \sum_{j\in\mathcal{N}_i} (g_{ij}(t) - g^\star_{ij}) + k_v \sum_{j\in\mathcal{N}_i} \dot{g}_{ij}(t), \tag{4.2}$$

where k_p and k_v are positive position and velocity gains respectively, $\{g_{ij}\}_{(i,j)\in\mathcal{E}}$ are the relative bearings and $\{\dot{g}_{ij}\}_{(i,j)\in\mathcal{E}}$ are the rate of bearings. The closed-loop system is,

$$\dot{v}(t) = -k_p \bar{H}(g(t) - g^\star) - k_v \bar{H}\dot{g}(t). \tag{4.3}$$

As seen in [14], the system in (4.3) has an equilibrium when $g_{ij}(t) = g^\star_{ij},\ \dot{g}_{ij}(t) = 0$ and $v_i(t) = const \ \ i \in \mathcal{V}$, i.e., the final formation moves at a constant velocity.

However, since the focus of the latter half of this paper is to find an ETC for a stationary final formation, we propose the modified control law,

$$u_i(t) = k_p \sum_{j\in\mathcal{N}_i} (g_{ij}(t) - g^\star_{ij}) + k_v \sum_{j\in\mathcal{N}_i} \dot{g}_{ij}(t) - k_v v_i(t), \tag{4.4}$$

where $v_i \in \mathbb{R}^d$ is the velocity of agent i. In matrix form, the control law (4.4) is,

$$u(t) = -k_p \bar{H}(g(t) - g^\star) - k_v \bar{H}\dot{g}(t) - k_v v(t). \tag{4.5}$$

Before we provide the stability and convergence proof of the proposed controller (4.5), we present an assumption following our discussion in Section D.1 and introduce a lemma from [14]:

Assumption 4.1. Assume the target formation specified by the bearings $\{g^\star_{ij}\}_{(i,j)\in\mathcal{E}}$ is unique.

Lemma 4.1. *Suppose none of the agents coincide, i.e., $p_i \neq p_j \ \forall \ i,j \in \mathcal{V}$, then $p^T\bar{H}(g(t) - g^\star) \geq 0$ and equality exists if and only if $g(t) = g^\star$.*

Theorem 4.1. *Consider the dynamics in* (4.1) *under the action of control law* (4.4)*. Under Assumption 4.1, $g(t) \to g^\star$ and $v_i(t) \to 0$ as $t \to \infty$ for $i = 1, \cdots, n$, from any initial conditions, i.e., the system is globally asymptotically stable.*

Proof. Define $V : \mathbb{R}^{2nd} \to \mathbb{R}$, a continuously differentiable candidate Lyapunov function as,

$$V(p, v) = k_p p^T \bar{H}(g - g^\star) + \frac{1}{2} v^T v.$$

Using Lemma 4.1 and the norm property $v^T v > 0 \ \forall \ v \in \mathbb{R}^{nd} - \{0_{nd\times 1}\}$, we note that $V(p, v)$ is positive definite and radially unbounded since $V(p, v) \to \infty$ as $\| \begin{bmatrix} p^T & v^T \end{bmatrix} \| \to$

∞. It's time derivative is,

$$\dot{V}(p,v) = k_p(g-g^\star)^T\bar{H}^T v + k_p p^T \bar{H}\dot{g} + v^T\dot{v}, \tag{4.6}$$

and from the definition of the orthogonal projection matrix presented in Appendix D.1, we also have $e^T\dot{g} = 0$, giving us,

$$\begin{aligned}\dot{V}(p,v) &= k_p(g-g^\star)^T\bar{H}^T v + v^T\dot{v},\\ &= k_p(g-g^\star)^T\bar{H}^T v + v^T(-k_p\bar{H}(g-g^\star) - k_v\bar{H}\dot{g} - k_v v),\\ &= -k_v v^T\bar{H}\dot{g} - k_v v^T v,\\ &= -k_v v^T\bar{H}\mathrm{diag}\Big(\frac{P_{g_{ij}}}{\|e_{ij}\|}\Big)\bar{H}^T v - k_v v^T v\\ &= -k_v v^T\Big(\bar{H}\mathrm{diag}\Big(\frac{P_{g_{ij}}}{\|e_{ij}\|}\Big)\bar{H}^T + I\Big)v < 0,\end{aligned} \tag{4.7}$$

where the last inequality is due to $\mathrm{diag}\Big(\frac{P_{g_{ij}}}{\|e_{ij}\|}\Big)$ being positive-semi definite and hence $\Big(\bar{H}\mathrm{diag}\Big(\frac{P_{g_{ij}}}{\|e_{ij}\|}\Big)\bar{H}^T + I\Big)$ is positive definite. With the above Lyapunov function, we define a compact set $\Omega_a = \{(p,v) \in \mathbb{R}^{2nd} | V(p,v) \leq c\}$ and let $S = \{(p,v) \in \Omega_a | \dot{V} = 0\}$. From (4.7) we note that $\dot{V} = 0$ if and only if $v(t) = 0$ which implies the formation is stationary and hence $\dot{g}(t) = 0$. Additionally, $v(t) = 0 \Rightarrow \dot{v}(t) = 0$ and from (4.5) we obtain $-k_p\bar{H}(g(t) - g^\star) = 0$. Left multiplying this expression by p^T, we arrive at the result of Lemma 4.1 which is true if and only if $g(t) = g^\star$. The proof is complete by invoking Lyapunov's stability theorem. ■

4.2 Problem Statement

The control laws (4.2) and (4.4) are continuous time controllers. To design an event triggered scheme we need to define discontinuous states that exist only during the event times. These states are denoted by $\{\hat{g}_{ij}(t_i^k), \hat{\dot{g}}_{ij}(t_i^k)\}$ where t_i^k is the time when an event is triggered for agent i. The problem we study is when to use these discontinuous states and solve the bearing-based formation control problem, i.e., a problem where the final formation is specified by bearings between agents. We divide this problem into two sub-problems. In the first sub-problem we achieve bearing-based stabilization where the final formation is stationary and in the second sub-problem, we achieve bearing-based stabilization using only relative states where the final formation moves with a constant velocity. Formally, these two problems can be posed as follows:

Problem 4.1 Design an event-triggered condition for each agent $i \in \mathcal{V}$, that drives both the sensing and the control updates using the measured self states $\{p_i, v_i\}$ and the bearing states $\{g_{ij}, \dot{g}_{ij}\}$ such that $v_i \to 0\ \forall\ i \in \mathcal{V}$, $g_{ij} \to g_{ij}^\star$, $\dot{g}_{ij} \to 0$ for all $(i,j) \in \mathcal{E}$ as $t \to \infty$.

Problem 4.2 Design an event-triggered condition using continuously sensed relative measurements between agents $i, j \in \mathcal{V}$ that drives the control updates using the measured bearing states $\{g_{ij}, \dot{g}_{ij}\}$ and the measured relative velocities $\{\dot{e}_{ij}\}$ such that $g_{ij} \to g_{ij}^{\star}$ and $\dot{g}_{ij} \to 0$ for all $(i, j) \in \mathcal{E}$ as $t \to \infty$.

In Problem 4.2, we make use of the double-integrator control law (4.2) to arrive at an ETC that is dependent on the relative measurements between agents and we term such a problem as *edge triggering*. In Problem 4.1, along with the relative measurements, we use agents self states (p_i, v_i) in the double-integrator control law (4.4) to arrive at an ETC which is node dependent and will drive the agents to a stationary formation. We term this problem as *node triggering*.

4.3 Node Triggering

In this section, we design ETC for the node triggering case. As seen in Figure 4.1, the ETC is designed over each node and every agent has access to bearing measurements and its self states which is fed into the ETC. When this ETC is violated, the agent acquires new state measurements from its sensors, updates its controller and sets the error function to zero.

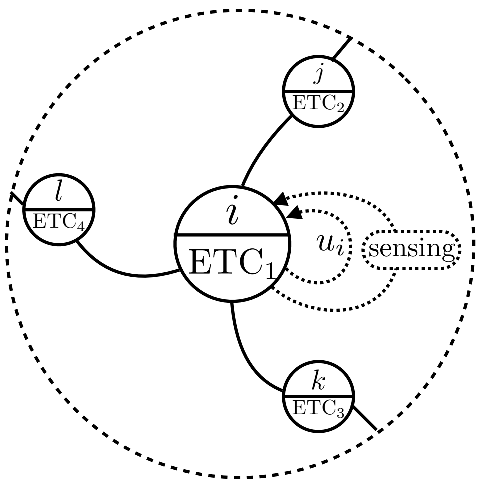

Figure 4.1: Illustration of node triggering ETC from the perspective of agent i.

4.3.1 Event-triggered Design

In node triggering, the sensing is discontinuous and driven by the ETC which is defined over the collective information acquired from all the neighbors of agent i. Here, the trigger response is not only to update the controller but also to drive the sensing of the neighboring states. The control law (4.4) is different from the one proposed in (4.2) as it uses self velocity of the agents to achieve a stationary final formation.

The error dynamics in this case are defined with respect to the position and velocity of the agents and are as follows,

$$r_{p_i}(t) \triangleq \hat{p}_i(t_i^k) - p_i(t) \quad \& \quad r_{v_i}(t) \triangleq \hat{v}_i(t_i^k) - v_i(t), \tag{4.8}$$

where $t \in [t_i^k, t_i^{k+1})$. The continuous controller in (4.4) is modified to the piecewise continuous controller,

$$u_i(t_i^k) = k_p \sum_{j \in \mathcal{N}_i} (\hat{g}_{ij}(t_i^k) - g_{ij}^\star) + k_v \sum_{j \in \mathcal{N}_i} \hat{\dot{g}}_{ij}(t_i^k) - k_v \hat{v}_i(t_i^k), \tag{4.9}$$

and the resulting closed-loop dynamics are,

$$\dot{v}_i(t) = k_p \sum_{j \in \mathcal{N}_i} (\hat{g}_{ij}(t_i^k) - g_{ij}^\star) + k_v \sum_{j \in \mathcal{N}_i} \hat{\dot{g}}_{ij}(t_i^k) - k_v \hat{v}_i(t_i^k). \tag{4.10}$$

The following theorem provides an ETC and presents convergence analysis for the system in (4.10):

Theorem 4.2. *Consider the system in* (4.1) *with control law* (4.10)*, assume the communication graph is undirected and connected, and that Assumption 4.1 holds. Suppose the ETC is given by,*

$$\|r_{v_i}\|^2 = \psi(t), \tag{4.11}$$

where

$$\psi(t) = \frac{2\epsilon}{k_v}\Big(\sigma\kappa\|v_i\|^2 - \frac{k_p}{2\epsilon}\|\sum_{j \in \mathcal{N}_i}(\hat{g}_{ij} - g_{ij}^\star)\|^2 - \frac{k_v}{2\epsilon}\|\sum_{j \in \mathcal{N}_i}\hat{\dot{g}}_{ij}\|^2\Big), \tag{4.12}$$

r_{v_i} *is the sensing error in velocity as defined in* (4.8)*,* $\epsilon > 0$*, and* $\kappa = k_v(1-\epsilon) - \frac{k_p\epsilon}{2}$*. Then for* $\sigma \in (0,1)$*, and for any initial conditions, the above ETC decides when to generate the control input* $u_i(t_i^k)$ *and when to measure the self- and bearing-states such that* $\hat{v}_i(t_i^k) \to 0$*,* $\hat{g}_{ij}(t_i^k) \to g_{ij}^\star$*, and* $\hat{\dot{g}}_{ij}(t_i^k) \to 0$*, where* $g_{ij}^\star$ *is the final bearing requirement to achieve the desired formation. Furthermore, the inter-event times* $(t_i^{k+1} - t_i^k)$ *are lower bounded by a* Δ *given by,*

$$\Delta = (1/\alpha)\log\left(1 + \frac{\alpha^2\psi(t)}{\|u_i(t_i^k)\|^2}\right), \tag{4.13}$$

where $\alpha > 0$*.*

Proof. Define $V : \mathbb{R}^{2nd} \to \mathbb{R}$ as $V(p_i, v_i) = \sum_{i=1}^n \frac{1}{2} v_i^T v_i$. The function is a continuously differentiable function on the set $\Omega_c = \{(p,v) \in \mathbb{R}^{2nd} | V(p,v) \leq const.\}$ which is positively invariant to (4.1). Its time derivative is,

$$\dot V(p,v) = \sum_{i=1}^{n} v_i^T \dot v_i = \sum_{i=1}^{n} v_i^T \Big(k_p \sum_{j\in\mathcal{N}_i} (\hat g_{ij} - g_{ij}^\star) + k_v \sum_{j\in\mathcal{N}_i} \hat{\dot g}_{ij} - k_v \hat v_i \Big)$$

$$= \sum_{i=1}^{n} v_i^T \Big(k_p \sum_{j\in\mathcal{N}_i} (\hat g_{ij} - g_{ij}^\star) + k_v \sum_{j\in\mathcal{N}_i} \hat{\dot g}_{ij} - k_v (v_i + r_{v_i}) \Big).$$

Using the error definitions of (4.8) and Young's inequality for inner products defined in Appendix A,we bound the above equation as,

$$\dot V(p,v) \le \sum_{i=1}^{n} \Big[k_p \Big(\frac{\epsilon \|v_i\|^2}{2} + \frac{\| \sum_{j\in\mathcal{N}_i} (\hat g_{ij} - g_{ij}^\star)\|^2}{2\epsilon} \Big) +$$

$$k_v \Big(\frac{\epsilon \|v_i\|^2}{2} + \frac{\| \sum_{j\in\mathcal{N}_i} \hat{\dot g}_{ij}\|^2}{2\epsilon} \Big) - k_v \|v_i\|^2 + k_v \Big(\frac{\epsilon \|v_i\|^2}{2} + \frac{\|r_{v_i}\|^2}{2\epsilon} \Big) \Big].$$

Restricting $\|r_{v_i}\|^2$ above to,

$$\|r_{v_i}\|^2 \le \psi(t), \tag{4.14}$$

with $\psi(t)$ given in (4.12), results in,

$$\dot V(p,v) \le \sum_{i=1}^{n} (\sigma - 1)\kappa k_v \|v_i\|^2,$$

which is negative semi-definite for $\sigma \in (0,1)$ and $\kappa = k_v(1-\epsilon) - \frac{k_p \epsilon}{2} > 0$. Invoking the invariance principle, [41], define $S_2 = \{(p,v) \in \mathbb{R}^{2nd} | \dot V = 0\}$. Then $\dot V = 0$ implies $v_i = 0$, which implies $\dot e_{ij} = 0$ and $\dot g_{ij} = 0$. From (4.10) we arrive at $k_p \sum_{j\in\mathcal{N}_i} (\hat g_{ij} - g_{ij}^\star) = 0$. This is satisfied only when $\hat g_{ij} = g_{ij}^\star$ which follows from Lemma 4.1.

The next event time for system (4.10) is,

$$t_i^{k+1} = t_i^k + \inf \Big\{ t \mid \|r_{v_i}\|^2 = \psi(t) \Big\},$$

and the above sequence of triggering instants $\{t_i^k\}_{k=0}^{\infty}$ is practically feasible only if we can find a lower bound between two successive triggering instants. The inter-event time $\Delta = t_i^{k+1} - t_i^k$ is the time taken for the error term $\|r_{v_i}\|$ to rise from 0 to the threshold present in (4.11) as discussed in [57]. For $t \in [t_i^k, t_i^{k+1})$,

$$\frac{\mathrm{d}}{\mathrm{d}t} r_{v_i}^T r_{v_i} = 2 r_{v_i}^T (-\dot v_i) \le \Big(\alpha \|r_{v_i}\|^2 + (1/\alpha)\|u_i\|^2 \Big),$$

where we used the Young's inequality for inner products. Denoting $y = \|r_{v_i}\|^2$, we obtain $\dot y \le \alpha y + (1/\alpha)\|u_i\|^2$ and y satisfies $y(t) \le \phi(t)$ where $\phi(t)$ is the solution of $\dot\phi - \alpha\phi = (1/\alpha)\|u_i\|^2$. The solution to this equation is,

$$\phi(t) = (1/\alpha^2)\|u_i\|^2 (\exp(\alpha(t - t_i^k)) - 1),$$

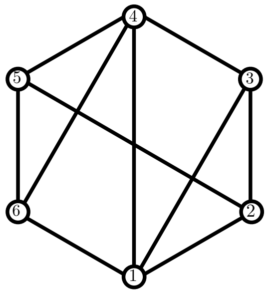

$$g_{12}^{\star} = \begin{bmatrix} \sqrt{3}/2 & 1/2 \end{bmatrix}^T \quad g_{61}^{\star} = \begin{bmatrix} \sqrt{3}/2 & -1/2 \end{bmatrix}^T$$
$$g_{23}^{\star} = \begin{bmatrix} 0 & 1 \end{bmatrix}^T \quad g_{13}^{\star} = \begin{bmatrix} 1/2 & \sqrt{3}/2 \end{bmatrix}^T$$
$$g_{34}^{\star} = \begin{bmatrix} -\sqrt{3}/2 & 1/2 \end{bmatrix}^T \quad g_{14}^{\star} = \begin{bmatrix} 0 & 1 \end{bmatrix}^T$$
$$g_{45}^{\star} = \begin{bmatrix} -\sqrt{3}/2 & -1/2 \end{bmatrix}^T \quad g_{25}^{\star} = \begin{bmatrix} -\sqrt{3}/2 & 1/2 \end{bmatrix}^T$$
$$g_{56}^{\star} = \begin{bmatrix} 0 & -1 \end{bmatrix}^T \quad g_{46}^{\star} = \begin{bmatrix} -1/2 & -\sqrt{3}/2 \end{bmatrix}^T$$

Figure 4.2: Communication graph for the example.

where $t \in [t_i^k, t_{i+1}^k)$. Now using the equality (4.11), we arrive at the following bound for inter-event times,

$$t - t_i^k \geq (1/\alpha) \log \left(1 + \frac{\alpha^2 \psi(t)}{\|u_i(t_i^k)\|^2} \right),$$

where $\psi(t)$ is given in (4.12).

Remark. While providing a lower bound on the inter-event times does not exclude Zeno behavior, we note that in numerous simulations we do not observe this phenomenon.

4.3.2 Simulation Results

The simulation results of Section 4.3.1 are presented here. We demonstrate the effectiveness of the theoretical results presented in Section 4.3 by simulating an example for a network of 6 agents with communication topology as shown in Figure 4.2.

In node triggering, the agents in Figure 4.2 are simulated with position and velocity gains $k_p = 8$ and $k_v = 4$ respectively. The initial conditions are random and the event variable σ is specified as 0.5.

In Figure 4.3a we observe that the desired formation is achieved with a convergence time of $t_f = 32.28s$, a final bearing error of 0.07 and the final formation is stationary as concluded from the discussions in Theorem 4.2. It needs to be pointed that along with control updates, the sensing is also event driven here. Figure 4.3b shows the instances when an event is triggered using the ETC (4.14). Here, every marker represents an instance when an agent updates its controller and acquires new bearing-state measurements. The evolution of bearing error, defined as $\sum_{(i,j)\in\mathcal{E}} \|g_{ij} - g_{ij}^{\star}\|$ is shown in Figure 4.3c and the lower bound for the inter-event time calculated for agent 2 using (4.13) and the actual inter-event time is shown in Figure 4.3d. Here we confirm the findings that the actual inter-event time is indeed lower bounded by Δ presented in (4.13).

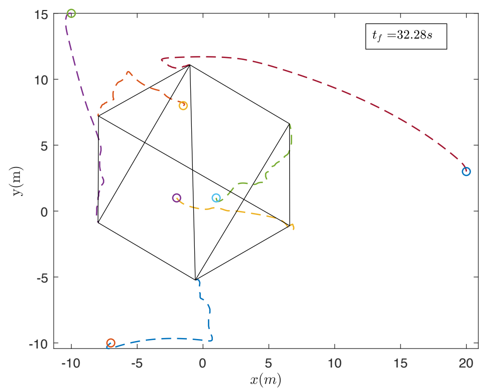

(a) Formation trajectory for the control law (4.10) and event condition (4.14).

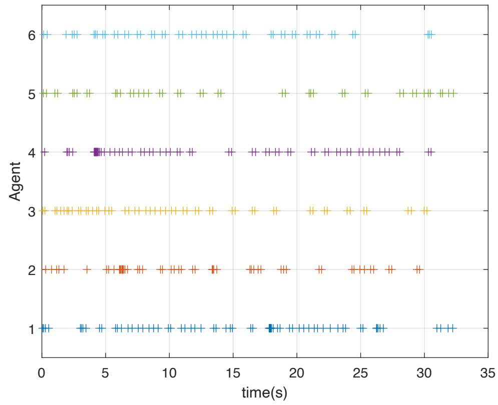

(b) Event triggering instances for agents shown in Figure 4.2.

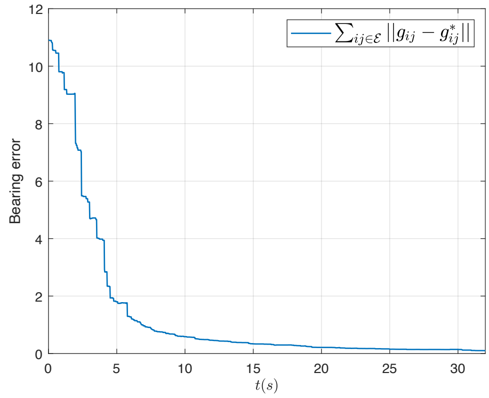

(c) Evolution of bearing error defined by $\sum_{(i,j)\in\mathcal{E}} \|g_{ij} - g_{ij}^\star\|$.

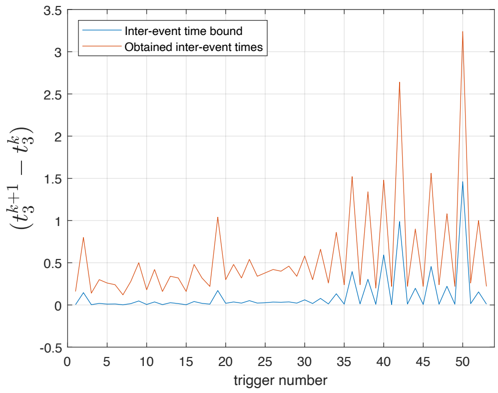

(d) Comparison of inter-event times for the bounds calculated in (4.13).

Figure 4.3: Results pertaining to the node-triggering case

4.4 Edge Triggering

In Section 4.3.1 we designed conditions when trigger conditions are evaluated on the states of each agent. In this section, the event-triggered conditions are dependent on the information from each edge - that is relative state information and measurements between neighboring agents. This can be well understood by observing Figure 4.4. In traditional event-triggered schemes, agent i monitors the states of all its neighbors and uses this aggregated information to evaluate an ETC. However, in edge triggering, we define the error dynamics on the relative bearings and rate of bearings. This means that execution of a trigger response is no longer dependent on the states of all the neighbors but on each edge. Edge $(i, j) \in \mathcal{E}$ has its trigger condition evaluated by agent i and agent j and if violated, the bearings and rate of bearings of that particular edge is updated and a new control input is generated. Assuming perfect information, agent i and agent j trigger events at the same time. To summarize, ETC drives control updates in edge triggering and ETC drives both sensing and control updates in node triggering. The total number of event-triggered conditions to be evaluated here is $2|\mathcal{E}|$

whereas node triggering network evaluates $|\mathcal{V}| = n$ conditions.

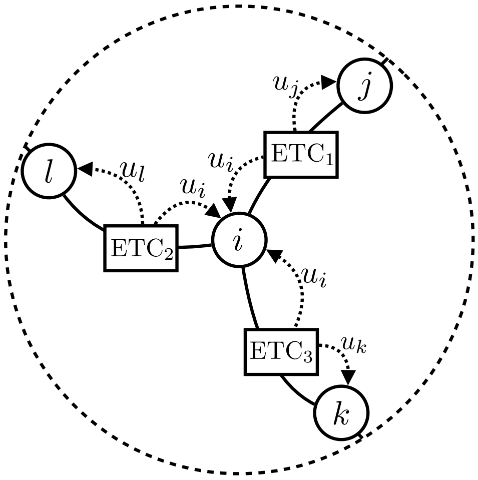

Figure 4.4: Illustration of edge triggering ETC from the perspective of agent i.

4.4.1 Event-triggered Design

The aim of designing an ETC is to derive a threshold function which dictates how far the error function can be allowed to rise before requiring an update, i.e., how far the states of the system can evolve without updating the controller. These updates occur at event times denoted by $t_i^1, t_i^2, \ldots$, and the control input between events is held constant in a zero-order hold fashion. The bearing states that exist at event times are denoted by $\{\hat{g}_{ij}, \hat{\dot{g}}_{ij}\}$ and are constant between the interval $[t_i^k, t_i^{k+1})$. To check how far the bearing states have evolved in this interval, we define time-dependent error terms $r_{g_{ij}}(t)$ and $r_{\dot{g}_{ij}}(t)$. Using this information, the relative errors are as follows,

$$r_{g_{ij}}(t) \triangleq \hat{g}_{ij}(t_i^k) - g_{ij}(t) \ \& \ r_{\dot{g}_{ij}}(t) \triangleq \hat{\dot{g}}_{ij}(t_i^k) - \dot{g}_{ij}(t), \tag{4.15}$$

where $t \in [t_i^k, t_i^{k+1})$. Using the above notations, we can modify the continuous controller (4.2) to a piecewise continuous controller by replacing the states $\{g_{ij}, \dot{g}_{ij}\}$ with $\{\hat{g}_{ij}, \hat{\dot{g}}_{ij}\}$ and the resulting closed-loop dynamics are,

$$\dot{v}_i(t_i^k) = k_p \sum_{j \in \mathcal{N}_i} (\hat{g}_{ij}(t_i^k) - g_{ij}^{\star}) + k_v \sum_{j \in \mathcal{N}_i} \hat{\dot{g}}_{ij}(t_i^k). \tag{4.16}$$

The following result provides convergence analysis for the system (4.16):

Theorem 4.3. *Consider the system in* (4.1) *with control law* (4.16) *and assume the communication graph is undirected and that Assumption 4.1 holds. Suppose the event-triggered condition is given by,*

$$k_p \|\dot{e}_{ij}\| \|r_{g_{ij}}\| + k_v \|\dot{e}_{ij}\| \|r_{\dot{g}_{ij}}\| = \sigma k_v \langle \dot{e}_{ij}, \dot{g}_{ij} \rangle, \tag{4.17}$$

where $\sigma \in (0,1)$ *is a design parameter,* $\dot{e}_{ij}$ *is the relative velocity,* $r_{g_{ij}}$ *is the sensing error in* $\{g_{ij}\}_{j\in N_i}$ *and* $r_{\dot{g}_{ij}}$ *is the sensing error in* $\{\dot{g}_{ij}\}_{j\in N_i}$ *as defined in* (4.15)*. Then for any initial conditions, the ETC in* (4.17) *decides when to generate the control update* $u_i(t_i^k)$ *such that* $\dot{g}_{ij}(t) \to 0$ *and* $g_{ij}(t) \to g_{ij}^\star$*, where* $g_{ij}^\star$ *is the final bearing requirement to achieve the desired formation.*

Remark. The ETC in (4.17) makes use of the relative bearing states $\{g_{ij}, \dot{g}_{ij}\}$ and the relative velocities $\{\dot{e}_{ij}\}$.

Proof. Define $V : \mathbb{R}^{2nd} \to \mathbb{R}$, a continuously differentiable function on the set $\Omega_b = \{(p,v) \in \mathbb{R}^{2nd} | V(p,v) \leq const.\}$ which is positively invariant to (4.1) as $V(p,v) = k_p e^T(g - g^\star) + \frac{1}{2}v^T v$. whose time derivative is,

$$\begin{aligned}
\dot{V}(p,v) &= k_p(g-g^\star)^T \bar{H}^T v + v^T \dot{v}, \\
&= k_p(g-g^\star)^T \bar{H}^T v + v^T(-k_p \bar{H}(\hat{g}-g^\star) - k_v \bar{H}\hat{\dot{g}}), \\
&= k_p(g-g^\star)^T \bar{H}^T v - k_p v^T \bar{H}(\hat{g}-g^\star) - k_v v^T \bar{H}\hat{\dot{g}}, \\
&= k_p\langle g-g^\star, \bar{H}^T v\rangle - k_p\langle \hat{g}-g^\star, \bar{H}^T v\rangle - k_v v^T \bar{H}\hat{\dot{g}}, \\
&= k_p\langle \hat{g}-r_g-g^\star, \bar{H}^T v\rangle - k_p\langle \hat{g}-g^\star, \bar{H}^T v\rangle - k_v v^T \bar{H}\hat{\dot{g}}, \\
&= -k_p v^T \bar{H} r_g - k_v v^T \bar{H}\hat{\dot{g}} = -k_p \dot{e}^T r_g - k_v \dot{e}^T r_{\dot{g}} - k_v \dot{e}^T \dot{g}, \\
&= -k_p \sum_i \sum_{j\in N_i} \langle \dot{e}_{ij}, r_{g_{ij}}\rangle - k_v \sum_i \sum_{j\in N_i} \langle \dot{e}_{ij}, r_{\dot{g}_{ij}}\rangle - k_v \sum_i \sum_{j\in N_i} \langle \dot{e}_{ij}, \dot{g}_{ij}\rangle,
\end{aligned}$$

which follows from the property that $e_{ij}^T \dot{g}_{ij} = 0$ and the error definitions from (4.15). Using Cauchy-Schwarz inequality $|\langle a,b\rangle| \leq \|a\|\|b\|$, we bound the above equation as,

$$\dot{V}(p_i,v_i) \leq k_p \sum_i \sum_{j\in N_i} \|\dot{e}_{ij}\|\|r_{g_{ij}}\| + k_v \sum_i \sum_{j\in N_i} \|\dot{e}_{ij}\|\|r_{\dot{g}_{ij}}\| - k_v \sum_i \sum_{j\in N_i} \langle \dot{e}_{ij}, \dot{g}_{ij}\rangle.$$

To ensure the above derivative is negative semi-definite, we will enforce,

$$k_p\|\dot{e}_{ij}\|\|r_{g_{ij}}\| + k_v\|\dot{e}_{ij}\|\|r_{\dot{g}_{ij}}\| \leq \sigma k_v \langle \dot{e}_{ij}, \dot{g}_{ij}\rangle, \tag{4.18}$$

where we again used the Cauchy-Schwarz inequality and this condition ensures that the following derivative of the Lyapunov function,

$$\dot{V}(p_i,v_i) \leq (\sigma-1)k_v \sum_i \sum_{j\in N_i} \langle \dot{e}_{ij}, \dot{g}_{ij}\rangle,$$

is negative semi-definite for $\sigma \in (0,1)$. Invoking the Invariance principle, [41], define $S_1 = \{(p,v) \in \mathbb{R}^{2nd} | \dot{V} = 0\}$ where $\dot{V} = 0$ implies $\dot{e}_{ij}$ and $\dot{g}_{ij}$ are orthogonal to each other. As introduced in Appendix D, $\dot{g}_{ij}$ and g_{ij} are orthogonal to each other too (i.e., $\dot{g}_{ij}^T g_{ij} = 0$), then there exists a scalar γ, such that $\dot{e}_{ij} = \gamma g_{ij}$. Now from the definition of $\dot{g}_{ij}$, given by $\dot{g}_{ij} = \frac{\gamma P_{g_{ij}}}{\|e_{ij}\|} g_{ij}$, is 0 since $P_{g_{ij}}$ is the orthogonal projection of g_{ij} i.e., $P_{g_{ij}} g_{ij} = 0$.

Therefore $\dot{g}_{ij} = 0$ and $g_{ij}(t)$ is constant. At this point if $g_{ij} = g^{\star}_{ij}$ then the proof is complete and if $g_{ij} \neq g^{\star}_{ij}$ then $u(t^k_i)$ in (4.16) evolves until $g_{ij} = g^{\star}_{ij}$. ■

4.4.2 Simulation Results

The simulation results of Section 4.4 are presented here. We demonstrate the effectiveness of the theoretical results presented in Section 4.3 by simulating an example for a network of 6 agents with communication topology as shown in Figure 4.2. For the system with dynamics (4.1) with control law (4.16) and under the action of ETC (4.18), as noticed in Figure 4.5a all 6 agents achieve the desired formation and continue moving and scaling with a constant final velocity. The snapshots of agents at $t = 20s, 40s$ and $t = 60s$ are also shown in Figure 4.5a. As discussed in Assumption 4.1, the framework is infinitesimal bearing rigid and the only trivial motion observed here is scaling.

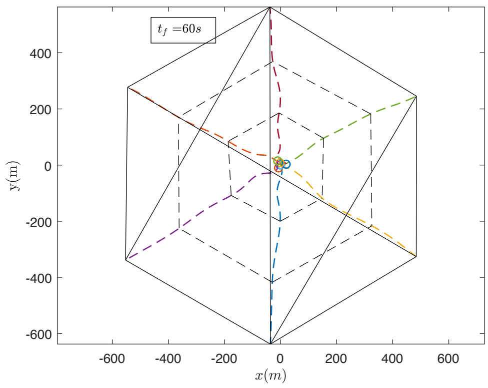

(a) Formation trajectory for the control law (4.16) and event condition (4.18).

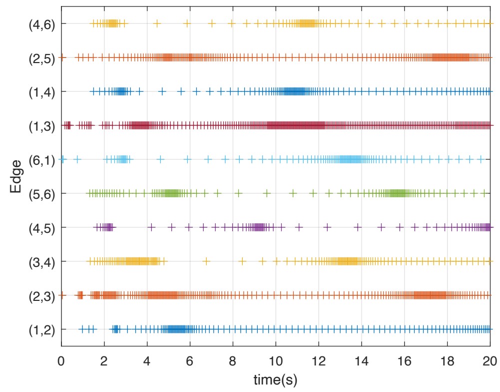

(b) Event triggering instances for agents shown in Figure 4.2.

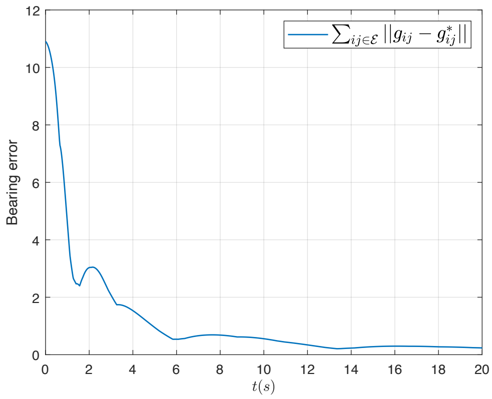

(c) Evolution of bearing error defined by $\sum_{(i,j)\in\mathcal{E}} \|g_{ij} - g^{\star}_{ij}\|$.

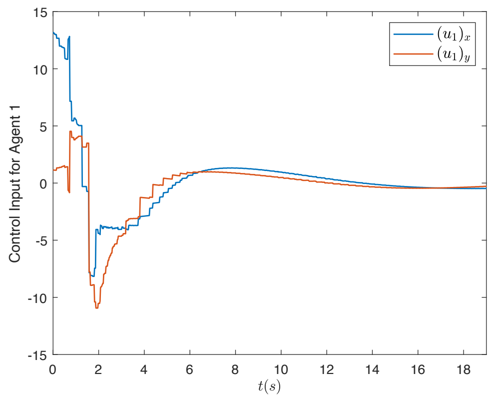

(d) Control input for agent 1 defined in (4.16).

Figure 4.5: Results pertaining to the edge-triggering case

Figure 4.5b shows the instances when an event is triggered over a particular edge and every marker over an edge $(i, j) \in \mathcal{E}$ indicates a control update for agent i and agent j. The evolution of bearing error as seen in Figure 4.5c is smooth unlike the bearing error in Figure 4.3c. This is because the sensing is continuous in edge triggering unlike

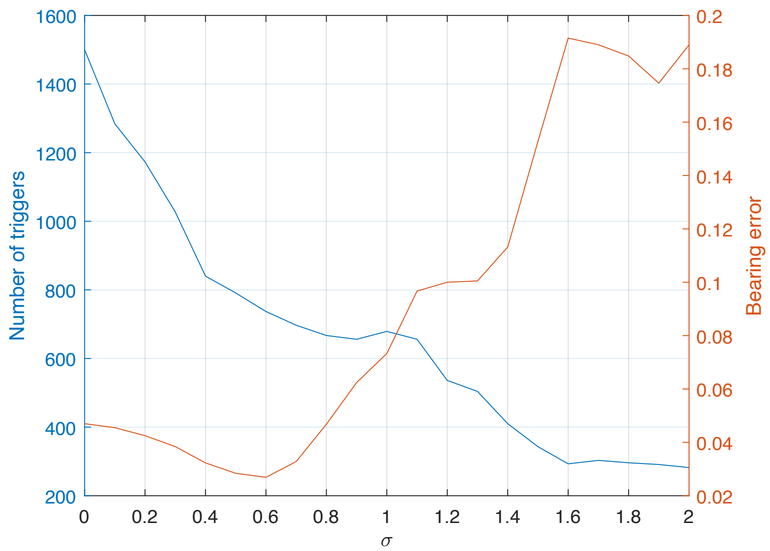

Figure 4.6: Dependence of convergence on σ.

the node triggering case. The control command for agent 1 from (4.16) is shown in Figure 4.5d and as noted earlier, the control and hence actuation is piecewise continuous thereby providing us better resource efficiency. In Figure 4.6, we see the dependence of number of triggers and convergence accuracy on the design variable σ. As discussed in Theorem 4.3, we need to restrict $\sigma \in (0, 1)$, however from Figure 4.6 we observe that σ can be greater than 1 by slowing the convergence rate, which also says that ETC's are quite conservative in most cases.

4.5 Alternative Edge Triggering

As discussed in Chapter 2, event-triggering conditions are not unique. In this section, we present an alternate edge-triggering condition. To start with, denote the directed edge $(i, j) \in \mathcal{E}$ by $k \in \{1, 2, \ldots, |\mathcal{E}|\}$. The edge vectors for kth edge are,

$$e_k = e_{ij} = p_j - p_i, \quad \dot{e}_k = \dot{e}_{ij} = v_j - v_i,$$

and the bearing vectors are,

$$g_k = g_{ij} = \sigma \frac{e_k}{\|e_k\|}, \quad \dot{g}_k = \dot{g}_{ij} = \frac{P_{g_k} \dot{e}_k}{\|e_k\|}.$$

The following theorem presents an event-triggering condition for the edge triggering case that is different from the one presented in Theorem 4.3,

Theorem 4.4. *Consider the system in* (4.1) *with control law* (4.16) *and assume the communication graph is undirected and that Assumption 4.1 holds. Suppose the event-*

triggered condition is given by,

$$k_v \|\dot{e}_{ij}\| \|r_{\dot{g}_{ij}}\| = \sigma k_v \dot{e}_{ij} \dot{g}_{ij} + k_p \dot{e}_{ij} (\hat{g}_{ij} - g^{\star}_{ij}), \tag{4.19}$$

where $\sigma \in (0,1)$ is a design parameter, $\dot{e}_{ij}$ is the relative velocity, $r_{g_{ij}}$ is the sensing error in $\{g_{ij}\}_{j\in N_i}$ and $r_{\dot{g}_{ij}}$ is the sensing error in $\{\dot{g}_{ij}\}_{j\in N_i}$ as defined in (4.15)*. Then for any initial conditions, the ETC in* (4.17) *decides when to generate the control update $u_i(t_i^k)$ such that $\dot{g}_{ij}(t) \to 0$ and $g_{ij}(t) \to g^{\star}_{ij}$, where $g^{\star}_{ij}$ is the final bearing requirement to achieve the desired formation.*

Remark. The ETC in (4.19) makes use of the relative bearing states $\{g_{ij}, \dot{g}_{ij}\}$ and the relative velocities $\{\dot{e}_{ij}\}$.

Proof. Define $V : \mathbb{R}^{2nd} \to \mathbb{R}$, a continuously differentiable function on the set $\Omega_b = \{(p,v) \in \mathbb{R}^{2nd} | V(p,v) \leq const.\}$ which is positively invariant to (4.1) as

$$V(p,v) = \sum_{k\in\mathcal{E}} \dot{e}_k^T \dot{e}_k,$$

whose time derivative is,

$$\begin{aligned}
\dot{V}(p,v) &= \sum_{k\in\mathcal{E}} \dot{e}_k^T \ddot{e}_k = \dot{e}^T \ddot{e} = (v^T \bar{H})(\bar{H}^T \dot{v}), \\
&= v^T \bar{H}\bar{H}^T (-k_p \bar{H}(\hat{g} - g^{\star}) - k_v \bar{H}\hat{\dot{g}}), \\
&= -k_p (v^T \bar{H}\bar{H}^T) \bar{H}(\hat{g} - g^{\star}) - k_v (v^T \bar{H}\bar{H}^T) \bar{H}\hat{\dot{g}},
\end{aligned}$$

where $\bar{H}\bar{H}^T = \bar{L} = L \otimes I_d$ where L is the Laplacian matrix. The vector $v^T \bar{L}$ is then $\sum_{j\in\mathcal{N}_i}(v_j - v_i) = \sum_{j\in\mathcal{N}_i} \dot{e}_{ij}$ for $i \in \mathcal{V}$. Using these we expand the expression for $\dot{V}(p,v)$ as follows,

$$\begin{aligned}
\dot{V}(p,v) = &- k_p \begin{bmatrix} \sum_{j\in\mathcal{N}_1} \dot{e}_{1j}^T & \sum_{j\in\mathcal{N}_2} \dot{e}_{2j}^T & \dots & \sum_{j\in\mathcal{N}_n} \dot{e}_{nj}^T \end{bmatrix} \begin{bmatrix} \sum_{k\in\mathcal{N}_1} (\hat{g}_{1k} - g^{\star}_{1k}) \\ \sum_{k\in\mathcal{N}_2} (\hat{g}_{2k} - g^{\star}_{2k}) \\ \dots \\ \sum_{k\in\mathcal{N}_n} (\hat{g}_{nk} - g^{\star}_{nk}) \end{bmatrix} \\
&- k_v \begin{bmatrix} \sum_{j\in\mathcal{N}_1} \dot{e}_{1j}^T & \sum_{j\in\mathcal{N}_2} \dot{e}_{2j}^T & \dots & \sum_{j\in\mathcal{N}_n} \dot{e}_{nj}^T \end{bmatrix} \begin{bmatrix} \sum_{k\in\mathcal{N}_1} \hat{\dot{g}}_{1k} \\ \sum_{k\in\mathcal{N}_2} \hat{\dot{g}}_{2k} \\ \vdots \\ \sum_{k\in\mathcal{N}_n} \hat{\dot{g}}_{nk} \end{bmatrix},
\end{aligned}$$

which can be summed as follows,

$$\begin{aligned}\dot{V}(p,v) &= -k_p \sum_i \sum_{j\in\mathcal{N}_i} \sum_{k\in\mathcal{N}_i} \dot{e}_{ij}(\hat{g}_{ik} - g^\star_{ik}) - k_v \sum_i \sum_{j\in\mathcal{N}_i} \sum_{k\in\mathcal{N}_i} \dot{e}_{ij}(\dot{\hat{g}}_{ik}) \\
&= -k_p \sum_i \sum_{j\in\mathcal{N}_i} \sum_{k\in\mathcal{N}_i} \dot{e}_{ij}(\hat{g}_{ik} - g^\star_{ik}) - k_v \sum_i \sum_{j\in\mathcal{N}_i} \sum_{k\in\mathcal{N}_i} \dot{e}_{ij}(\dot{g}_{ik} + r_{\dot{g}_{ik}}) \\
&= -k_p \sum_i \sum_{j\in\mathcal{N}_i} \sum_{k\in\mathcal{N}_i} \dot{e}_{ij}(\hat{g}_{ik} - g^\star_{ik}) - k_v \sum_i \sum_{j\in\mathcal{N}_i} \sum_{k\in\mathcal{N}_i} \dot{e}_{ij}\dot{g}_{ik} - k_v \sum_i \sum_{j\in\mathcal{N}_i} \sum_{k\in\mathcal{N}_i} \dot{e}_{ij} r_{\dot{g}_{ik}} \\
&\leq -k_p \sum_i \sum_{j\in\mathcal{N}_i} \sum_{k\in\mathcal{N}_i} \dot{e}_{ij}(\hat{g}_{ik} - g^\star_{ik}) - k_v \sum_i \sum_{j\in\mathcal{N}_i} \sum_{k\in\mathcal{N}_i} \dot{e}_{ij}\dot{g}_{ik} + k_v \sum_i \sum_{j\in\mathcal{N}_i} \sum_{k\in\mathcal{N}_i} \|\dot{e}_{ij}\|\|r_{\dot{g}_{ik}}\|,\end{aligned}$$

where we used the Cauchy-Schwarz inequality. Enforcing the following condition,

$$k_v\|\dot{e}_{ij}\|\|r_{\dot{g}_{ij}}\| \leq \sigma k_v \dot{e}_{ij}\dot{g}_{ij} + k_p \dot{e}_{ij}(\hat{g}_{ij} - g^\star_{ij}),$$

we arrive at the non-positive function,

$$\dot{V}(p,v) \leq (\sigma - 1) \sum_i \sum_{j\in\mathcal{N}_i} \sum_{k\in\mathcal{N}_i} \dot{e}_{ij}\dot{g}_{ij},$$

where $\sigma \in (0,1)$. The convergence conclusion is similar to that of Theorem 4.3. ■

The simulation results for the ETC (4.19) is shown below where we note that ETC (4.18) uses half the number of triggers used by ETC (4.19). The triggers from the condition (4.19) come in clusters as the term on the right of the inequality is sign indefinite. If $k_v \dot{e}_{ij}\dot{g}_{ij} + k_p \dot{e}_{ij}(\hat{g}_{ij} - g^\star_{ij})$ is negative then continuous triggers occur as $k_v\|\dot{e}_{ij}\|\|r_{\dot{g}_{ij}}\|$ is non-negative and (4.19) is always satisfied. This situation is avoided in (4.18) as the term on the right of the inequality is always non-negative.

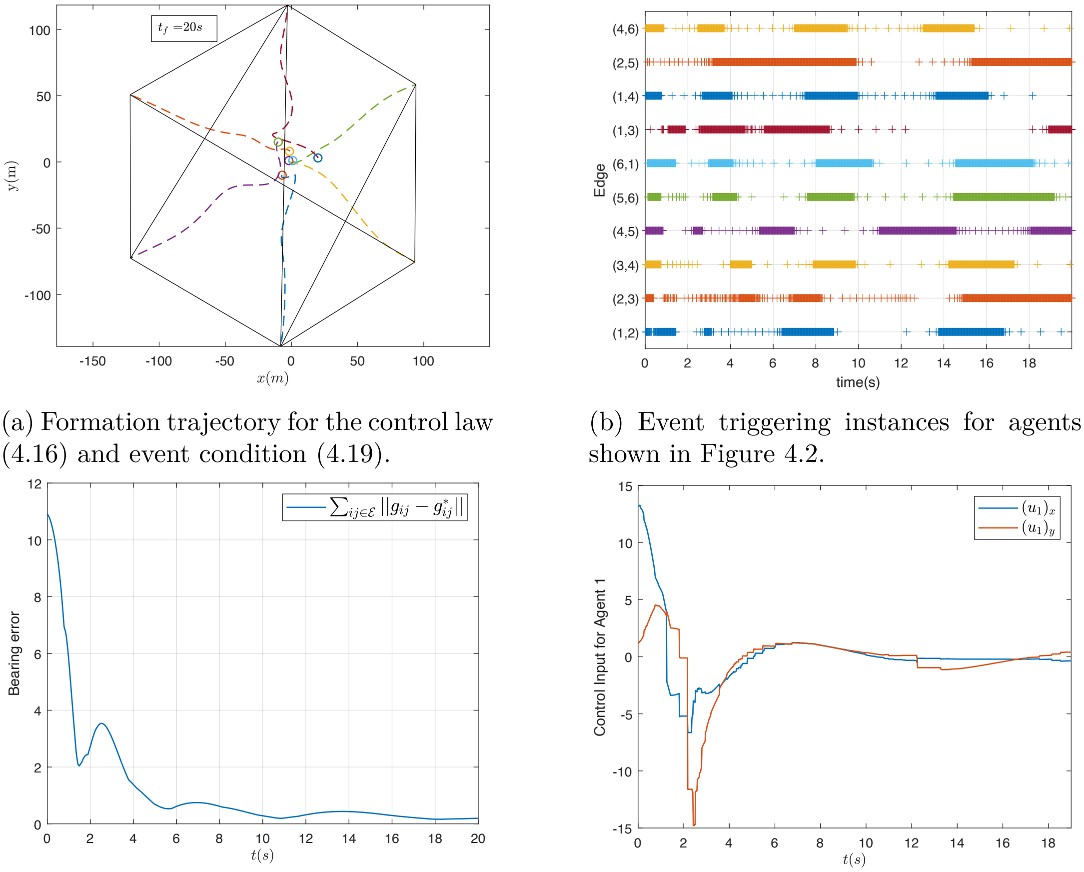

(a) Formation trajectory for the control law (4.16) and event condition (4.19).

(b) Event triggering instances for agents shown in Figure 4.2.

(c) Evolution of bearing error defined by $\sum_{(i,j)\in\mathcal{E}} \|g_{ij} - g^\star_{ij}\|$.

(d) Control input for agent 1 defined in (4.16).

Figure 4.7: Results pertaining to the alternative edge-triggering condition

Chapter 5

Closing Statement

In this Chpater we conclude the work presented and also discuss few directions for future research.

5.1 Conclusion

In Chapter 3 we solved the average and zero-velocity consensus problem by proposing a novel event triggered condition among a group of agents with double integrator dynamics. We highlight that the proposed condition relies only on relative state measurements and reduces the communication load on the system. The proposed event triggered scheme determined for each agent when to update its own states and when to broadcast its states when a locally computed error function exceeds a state-dependent threshold. We made use of a single ETC to solve two problems and lay emphasis on converting a consensus problem to a rendezvous problem by updating the controller in continuous time. In the average consensus problem, we used the ETC to direct the information exchange and the control updates of agents, whereas in the zero-velocity consensus problem we use the ETC to direct the information exchange between agents.

In Chapter 4, we presented distributed bearing-based event-triggered schemes to achieve formation stabilization for agents with double-integrator dynamics. We proposed two triggering mechanism that we term node triggering and edge triggering. When the only information available to agents are relative measurements, these measurements are a function of every edge and it is not possible to decouple them to obtain agents self-states. This lead to the notion of edge triggering, where we demonstrated how each edge can have its own ETC and drive the control updates of the agents. In node triggering, we used additional information in the form of self-velocity of agents to arrive at an ETC that uses collective information from all its neighbors to render the final formation stationary and ensures the inter-event times are strictly positive. We also presented a simulation example to establish the effectiveness of these results and showed that event-triggered control can substantially decrease the amount of processing power by sensing and updating controller at event times rather than traditional time-triggered updates.

5.2 Future Work

This thesis provides a foundation to answer plethora of future questions in the field. To start with, future work can be devoted to providing non-zeno proofs for the consensus problem and edge triggering problem. In the node triggering case, as presented in [45], even marginal disturbances can cause zeno-behavior which will warrant an analysis with time-delays, disturbances and noises. In the context of performance, one direction to look at is to find optimal sampling time for the proposed problems and compare them to the the event-triggered schemes presented. If the performance is not desired, approaches like dynamic event-triggering, team-triggering can be adopted or controller redesign can be considered such that certain performance bounds are enforced. The analysis can be followed in the lines of the one discussed in Part II of [58].

In another direction, experimental verification of the schemes will provide much needed validation for the implementation of event-triggered algorithms. Various dynamical models can be chosen to re-develop the problem in Chapter 3 and Chapter 4. Additionally, a more general gradient dynamical system analysis can be performed to cover the presented solutions into an umbrella of event-triggered conditions.

In the context of time-delayed systems, delay margins can be used to upper bound inter-event times to obtain non-conservative results. In another direction, as presented in [39] sometimes agents are better off by estimating the states of their neighbors if the dynamics of the entire system are identical and only request new information when such estimates deviate quickly. A trade-off study can be conducted to the impact on convergence rate, communication cost, computation resources required and inter-event times.

In Chapter 4, agents with limited field of view can be considered which would result in switching graph topology. In another direction, attacks on the triggering mechanism can be considered where the attacker controls the ETC switch and the switch can be kept open until the Lyapunov function gets unbounded thereby destabilizing the system. We discussed in Chapter 4 about designing ETC conditions over edges, a future direction can be to design these conditions over subgraphs and when an event is triggered the agents present in the subgraph share their states and update controllers which can minimize computation resources.

Appendix A

Basic Algebraic Notions

The Euclidean norm of $x = [x_1, x_2, \dots, x_n]^T$ on an n-dimensional Euclidean space $\mathbb{R}^n$ is given by $\|x\|_2 = \|x\| = \sqrt{x_1^2 + x_2^2 + \cdots + x_n^2}$. A matrix M is symmetric if $M = M^T$ i.e. the matrix is equal to its transpose. A symmetric real $n \times n$ matrix M is positive definite if the scalar $x^T M x$ is strictly positive and is positive semi-definite if the scalar $x^T M x$ is non-negative for $x \in \mathbb{R}^n / \mathbf{0}$. In terms of eigenvalues, M is positive definite if all its eigenvalues are positive and positive semi-definite if all its eigenvalues are non-negative. We can analogously define negative definiteness and negative semi-definiteness. The dot product of two vectors $x = [x_1, x_2, \dots, x_n]^T$ and $y = [y_1, y_2, \dots, y_n]^T$ is given by,

$$\langle x, y \rangle = x^T y = y^T x = \sum_{i=1}^{n} x_i y_i.$$

Next we present 3 inequalities from [54] that will come handy later on.

Definition A.1 (Young's inequality with ϵ). For any given $x, y \in \mathbb{R}$ and for $\epsilon \in \mathbb{R}_{>0}$, the following inequality holds,

$$|xy| \leq \frac{x^2}{2\epsilon} + \frac{\epsilon y^2}{2}.$$

The above inequality says, in order to gain tighter control on the second term one must loosen some control on the first term.

Definition A.2 (Cauchy-Schwarz inequality). This inequality states that for all vectors x and y of an inner product space it is true that,

$$|\langle x, y \rangle| \leq \langle x, x \rangle \cdot \langle y, y \rangle,$$

where $\langle \cdot, \cdot \rangle$ represents the inner product which in this work is a real dot product.

Definition A.3 (Triangle inequality). In a normed vector space S, the norm of the sum of two vectors is at most as large as the sum of the norms of the two vectors,

$$\|x + y\| \leq \|x\| + \|y\| \quad \forall\, x, y \in S.$$

Appendix B

Graph Theory

This section introduces concepts from graph theory that will be useful in the rest of the thesis. A graph $\mathcal{G}$ is a triplet $\mathcal{G} = (\mathcal{V}, \mathcal{E}, \mathcal{A})$ consisting of a finite vertex set $\mathcal{V} = \{w_1, w_2, \ldots, w_N\}$ with N vertices, an edge set $\mathcal{E} \subset \mathcal{V} \times \mathcal{V}$ and an adjacency matrix $\mathcal{A} \in \mathbb{R}_{>0}^{N\times N}$. The elements of adjacency matrix $a_{ij} = 1$ if $(w_i, w_j) \in \mathcal{E}$ and $a_{ij} = 0$ otherwise. The set of neighbors of vertex i is defined as,

$$\mathcal{N}_i = \{j \in \mathcal{V} : (w_i, w_j) \in \mathcal{E}\}.$$

The degree of a vertex, $d_i = \deg(w_i)$, for an undirected graph is the number of edges incident to the vertex w_i and the degree matrix Δ is a diagonal matrix where $[\Delta]_{ii} = d_i$. A graph is directed if each edge is assigned an orientation. An edge $(w_i, w_j) \in \mathcal{E}$ is directed from w_i to w_j if w_i is tail of the edge and w_j is head of the edge. An undirected graph is one where every edge is bi-directional, i.e., $(w_i, w_j) \in \mathcal{E}$ implies that $(w_j, w_i) \in \mathcal{E}$. A graph can also be represented by matrices which falls under the field of algebraic graph theory [59]. Some of the matrices are defined below.

- **Incidence matrix**: The incidence matrix of a graph $\mathcal{G}$ is the matrix $H(\mathcal{G})$ where,

$$[H(\mathcal{G})]_{ij} = \begin{cases} 1, & w_i \in \mathcal{V} \text{ is head of edge } e_j \in \mathcal{E}, \\ -1, & w_i \in \mathcal{V} \text{ is tail of edge } e_j \in \mathcal{E}, \\ 0, & \text{otherwise.} \end{cases}$$

- **Laplacian matrix**: The Laplacian matrix, L, which is of size $N \times N$ is defined as, $L = \Delta - \mathcal{A}$, and its elements are,

$$[L]_{ij} = \begin{cases} \deg(w_i) & \text{if } i = j \\ -1 & \text{if } i \neq j \text{ and } w_i \text{ is adjacent to } w_j \\ 0 & \text{otherwise.} \end{cases}$$

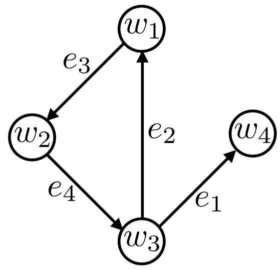

Figure B.1: A directed graph $\mathcal{G}_1$

The Laplacian matrix is also related to the incidence matrix as follows,

$$L = HH^T,$$

where for an undirected graph, L is a symmetric positive-semidefinite matrix. A matrix is positive-semidefinite if all the eigen-values of the matrix are non-negative. The eigenvalues of the Laplacian matrix satisfy the following inequality, $0 = \lambda_1 < \lambda_2 \leq \cdots \leq \lambda_N$. Consider the directed graph $\mathcal{G}_1$ in Figure B.1 whose Incidence and Laplacian matrix can be written as follows,

$$H(\mathcal{G}_1) = \begin{array}{c} \\ w_1 \\ w_2 \\ w_3 \\ w_4 \end{array} \begin{array}{c} \begin{array}{cccc} e_1 & e_2 & e_3 & e_4 \end{array} \\ \begin{bmatrix} 0 & 1 & -1 & 0 \\ 0 & 0 & 1 & -1 \\ -1 & -1 & 0 & 1 \\ 1 & 0 & 0 & 0 \end{bmatrix} \end{array},$$

and,

$$L = HH^T = \begin{bmatrix} 2 & -1 & -1 & 0 \\ -1 & 2 & -1 & 0 \\ -1 & -1 & 3 & -1 \\ 0 & 0 & -1 & 1 \end{bmatrix},$$

and its eigenvalues are $\lambda_1 = 0, \lambda_2 = 1, \lambda_3 = 3$ and $\lambda_4 = 4$ where we note that these are all non-negative due to the positive semi-definiteness of the Laplacian matrix.

Appendix C

Stability of Dynamical Systems

Consider the following autonomous system,

$$\dot{x} = f(x), \tag{C.1}$$

where $f : D \to \mathbb{R}^n$ is a locally Lipschitz map from a domain $D \subset \mathbb{R}^n$. Denote the equilibrium point of (C.1) as $\bar{x} \in D$ which means $f(\bar{x}) = 0$.

Definition C.1. The equilibrium $\bar{x}$ of (C.1) is,

- *stable* if, for each $\epsilon > 0$, there is a $\delta = \delta(\epsilon) > 0$ such that,

$$\|x(0)\| < \delta \implies \|x(t)\| < \epsilon, \quad \forall \;\; t \geq 0,$$

- *unstable* if it is not stable, and,
- *asymptotically stable* if it is stable and δ can be chosen such that,

$$\|x(0)\| < \delta \implies \lim_{t\to\infty} x(t) = \bar{x}.$$

The above stability definition says that if a trajectory originates in the δ neighborhood of $\bar{x}$ then it never leaves the ϵ neighborhood of $\bar{x}$, and the asymptotic stability says that any trajectory originating in the δ neighborhood will always converge to the point $\bar{x}$ as times tends to infinity, i.e., it converges asymptotically. Sometimes the point $\bar{x}$ is challenging to calculate analytically, in this scenario we make use of Lyapunov stability to judge the stability of (C.1). Lyapunov stability gives sufficient conditions for stability of (C.1) without having to actually solve the differential equation. Lyapunov stability can be used to show boundedness of the solution which makes it a very powerful tool in the analysis of event-triggered control systems. The following theorem provides conditions to determine if the given equilibrium is a globally asymptotically stable one.

Theorem C.1 (Lyapunov Direct Method)**.** *Let the origin $\bar{x} = 0$ be an equilibrium point for* (C.1) *and $D \subset \mathbb{R}^n$ a domain containing it. Let $V(x) : D \to \mathbb{R}$ be a continuously* *differentiable function such that,*

- $V(0) = 0$ *and* $V(x) > 0$, *in* $D - \{0\}$,
- $\dot{V}(x) \leq 0$, *in* D,

then $x(t) = 0$ *is stable. Moreover if*

$$\dot{V}(x) < 0 \quad in \quad D - \{0\}$$

then $x = 0$ *is asymptotically stable.*

Any function $V(x)$ satisfying the above conditions is called a Lyapunov function and the surface $V(x) = c$ for $c > 0$ is a Lyapunov surface. The above theorem summarizes to say if the condition $\dot{V}(x) \leq 0$ is satisfied then a trajectory starting in the Lyapunov surface $V(x) = c$ enters the set $\Omega_c = \{x \in \mathbb{R}^n | V(x) \leq c\}$ to never come out again. If further the condition $\dot{V}(x) < 0$ is satisfied then the trajectory crosses the level set $V(x) = c$ to enter a new level set $V(x) = c_1$ where $c_1 < c$ and the Lyapunov surface $V(x) = c_1$ keeps shrinking until it reaches the equilibrium point, i.e., the origin.

If only the condition $\dot{V}(x) \leq 0$ is satisfied then we cannot certainly say if the trajectory will reach the origin. However, if there exists a $V(x)$ whose derivative satisfies $\dot{V}(x) \leq 0$ in a domain about the origin, and if we can ascertain that no trajectory stays at points where $\dot{V}(x) = 0$ except at the origin, then the origin is asymptotically stable. If this domain is $\mathbb{R}^n$, then the origin is globally asymptotically stable. This concept is materialized in the proceding theorem of LaSalle called the *invariance principle*. Some definitions are introduced below before we state the LaSalle's invariance principle.

Definition C.2. A set M is an *invariant set* with respect to (C.1) if $x(0) \in M \implies x(t) \in M$ for all $t \in \mathbb{R}$.

Definition C.3. A set M is *positively invariant set* if $x(0) \in M \implies x(t) \in M$ for all $t \geq 0$.

Theorem C.2 (LaSalle's Invariance Principle)**.** *Let* $\Omega \subset D$ *be a compact set that is positively invariant with respect to* (C.1). *Let* $V : D \to \mathbb{R}$ *be a continuously differentiable function such that* $\dot{V}(x) \leq 0$ *in* Ω. *Let* E *be the set of all points in* Ω *where* $\dot{V}(x) = 0$. *Let* M *be the largest invariant set in* E. *Then every solution starting in* Ω *approaches* M *as* $t \to \infty$.

The proof of the above theorem follows from the argument that no solution $x(t)$ can stay in E other than the trivial solution $x(t) = 0$. This section was built on the results from [41, Chapter 4].

Appendix D

Bearing-based Formation Control

In this section we present an introduction to bearing-based formation control and is built on the results from [12] which applies bearing rigidity theory to arbitrary dimensional bearing-only formation stabilization problems.

D.1 Bearing Rigidity Theory

Bearing rigidity theory answers the following question: can a framework be uniquely determined up to a translation and a scaling factor using only bearing measurements? We start by defining an orthogonal projection matrix operator $P : \mathbb{R}^d \to \mathbb{R}^{d\times d}$ as,

$$P(x) = P_x \triangleq I_d - \frac{(xx^T)}{\|x\|^2},$$

where $x \in \mathbb{R}^d$ is a nonzero vector and $d \geq 2$ is the dimension of the cartesian space. The matrix P_x is positive-semi definite with one zero eigenvalue and $d-1$ eigenvalues at 1. A framework in $\mathbb{R}^d$ is a pair $(\mathcal{G}, p)$ that maps every vertex of a graph to a point in the space $\mathbb{R}^d$.

Definition D.1 (Bearing Equivalent Frameworks). Two frameworks $\mathcal{G}(p)$ and $\mathcal{G}(p')$ are bearing equivalent if $P_{p_i - p_j}(p'_i - p'_j) = 0$ for all $(i, j) \in \mathcal{E}$.

An example of bearing equivalent framework is shown in Figure D.1 where the bearings between $p(v_1)$ and $p(v_2)$ are equivalent in both the frameworks but the bearings between $p(v_1)$ and $p(v_3)$ are not equivalent. Similar arguments apply to points $p(v_4)$ and $p(v_3)$.

Definition D.2 (Bearing Congruent Frameworks). Two frameworks $\mathcal{G}(p)$ and $\mathcal{G}(p')$ are bearing congruent if $P_{p_i - p_j}(p'_i - p'_j) = 0$ for all $i, j \in \mathcal{V}$.

An example of bearing congruent framework is shown in Figure D.2 where the bearings between any two points is equivalent in both the frameworks and the only possible motions are trivial(translation and scaling).

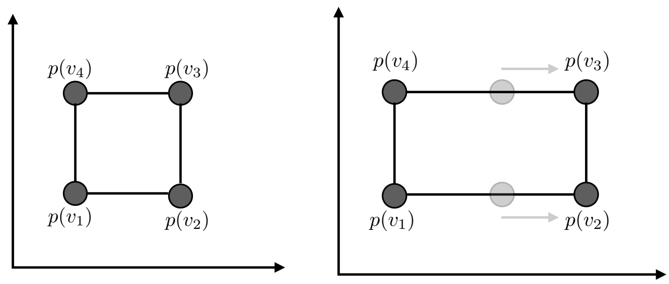

Figure D.1: Two equivalent but non-congruent frameworks $\mathcal{G}(p)$ and $\mathcal{G}(p')$

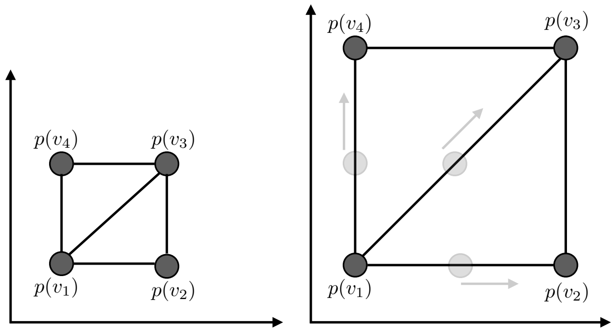

Figure D.2: Two congruent frameworks $\mathcal{G}(p)$ and $\mathcal{G}(p')$

All bearing congruent frameworks are bearing equivalent but the converse is not true. The relative position and velocity vectors between two agents (the *edge* vectors) are defined as,

$$e_{ij} \triangleq p_j - p_i, \quad \dot{e}_{ij} \triangleq v_j - v_i, \quad (i,j) \in \mathcal{E}.$$

The *bearing* and *rate of bearing* vector between two agents are defined as,

$$g_{ij} \triangleq \frac{e_{ij}}{\|e_{ij}\|}, \quad \dot{g}_{ij} \triangleq \frac{P_{g_{ij}}}{\|e_{ij}\|}\dot{e}_{ij}, \quad (i,j) \in \mathcal{E}.$$

The vectors e and $\dot{e}$ can thus be expressed in compact form as $e = \bar{H}^T p$ and $\dot{e} = \bar{H}^T v$. Since $P_{g_{ij}}$ is the orthogonal projection operator of g_{ij}, their inner product is 0, $P_{g_{ij}} g_{ij} = 0$. This also results in $g_{ij}^T \dot{g}_{ij} = e_{ij}^T \dot{g}_{ij} = 0$ and $\text{Null}(P_{g_{ij}}) = \text{span}\{g_{ij}\}$. The set of desired bearings are denoted by $\{g_{ij}^\star\}_{(i,j)\in\mathcal{E}}$.

We will now define the *bearing rigidity matrix* , denote the bearings of a directed edge as g_k where $k \in \{1, \ldots, m\}$ and define the bearing function $F_B : \mathbb{R}^{dn} \to \mathbb{R}^{dm}$ as, $F_B(p) \triangleq \left[g_1^T, \ldots, g_m^T\right]^T$. The *bearing rigidity matrix* is defined as the Jacobian of the bearing function,

$$R_B(p) \triangleq \frac{\partial F_B(p)}{\partial p} = \text{diag}\Big(\frac{P_{g_{ij}}}{\|e_{ij}\|}\Big)\bar{H}^T \in \mathbb{R}^{dm \times dn},$$

where $m = |\mathcal{E}|$ and $n = |\mathcal{V}|$. Let δp be a variation of p such that if $R_B(p)\delta p = 0$ then

δp is called an infinitesimal bearing motion. There are two kinds of trivial infinitesimal bearing motions: translation and scaling, which leads us to our next definition and assumption,

Definition D.3 (Unique Target Formation, [12]). A target formation can be uniquely determined if all the infinitesimal bearing motions are trivial.

The strongest notion of bearing rigidity is the infinitesimal bearing rigidity defined below.

Definition D.4 (Infinitesimal Bearing Rigidity). A framework is infinitesimal bearing rigid if the only allowable motions are translation and scaling of the entire framework.

For a framework $(\mathcal{G}, p)$ to be infinitesimally bearing rigid, it has to satisfy the following conditions listed below,

i) $\text{rank}(R(p)) = dn - d - 1$

ii) $\text{Null}(R(p)) = \text{span}\{\mathbb{1} \otimes I_d, p\}$.

Consider the framework in Figure D.3 which is the reproduction of Figure D.2 in $\mathbb{R}^2$ with arbitrary orientation. Its bearing rigidity matrix is built as follows, the incidence matrix is given by,

$$\bar{H} = \begin{bmatrix} -1 & 0 & 0 & 1 & -1 \\ 1 & -1 & 0 & 0 & 0 \\ 0 & 1 & -1 & 0 & 1 \\ 0 & 0 & 1 & -1 & 0 \end{bmatrix} \otimes \begin{bmatrix} 1 & 0 \\ 0 & 1 \end{bmatrix},$$

and the projection operator matrices for the 5 edges are,

$$P_{g_{12}} = P_{g_{34}} = \begin{bmatrix} 0 & 0 \\ 0 & 1 \end{bmatrix}, \quad P_{g_{23}} = P_{g_{34}} = \begin{bmatrix} 1 & 0 \\ 0 & 0 \end{bmatrix}, \quad P_{g_{13}} = \begin{bmatrix} 0.5 & -0.5 \\ -0.5 & 0.5 \end{bmatrix},$$

and the distance norms are, $\|e_{12}\| = \|e_{23}\| = \|e_{34}\| = \|e_{41}\| = 1$ and $\|e_{13}\| = \sqrt{2}$. The

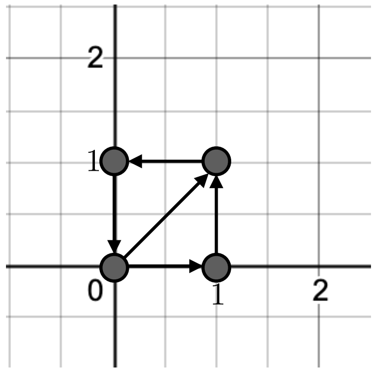

Figure D.3: An infinitesimally bearing rigid framework

bearing rigidity matrix can now be written as,

$$R(p) = \begin{bmatrix} 0 & 0 & 0 & 0 & 0 & 0 & 0 & 0 \\ 0 & -1 & 0 & 1 & 0 & 0 & 0 & 0 \\ 0 & 0 & -1 & 0 & 1 & 0 & 0 & 0 \\ 0 & 0 & 0 & 0 & 0 & 0 & 0 & 0 \\ 0 & 0 & 0 & 0 & 0 & 0 & 0 & 0 \\ 0 & 0 & 0 & 0 & 0 & -1 & 0 & 1 \\ 1 & 0 & 0 & 0 & 0 & 0 & -1 & 0 \\ 0 & 0 & 0 & 0 & 0 & 0 & 0 & 0 \\ -0.3536 & 0.3536 & 0 & 0 & 0.3536 & -0.3536 & 0 & 0 \\ 0.3536 & -0.3536 & 0 & 0 & -0.3536 & 0.3536 & 0 & 0 \end{bmatrix},$$

whose rank is 5 which equals $dn - d - 1 = 2(4) - 2 - 1 = 5$. Hence the framework in Figure D.3 is infinitesimally bearing rigid.

The event-triggered control theory developed in Chapter 4 assumes the formation to be infinitesimally bearing rigid and some necessary notions of bearing rigidity are also defined there.

D.2 Distributed Bearing-only Formation control

In this section we will provide results on bearing-only formation control of multi-agent systems from [12]. Consider the dynamics of each agents to be single-integrator,

$$\dot{p}_i(t) = v_i(t)$$

where $v_i(t) \in \mathbb{R}^d$ is the velocity input proposed as,

$$v_i(t) = -\sum_{j \in \mathcal{N}_i} P_{g_{ij}} g^\star_{ij}, \tag{D.1}$$

$\forall i \in \mathcal{V}$ and the constraints $\{g^\star_{ij}\}_{(i,j)\in\mathcal{E}}$ specify a final target formation.

Definition D.5 (Feasible Formation). A target formation is said to be *feasible* if there exists at least one configuration p that satisfies the bearing constraints, that is $g_{ij} = g^\star_{ij}$ for all $(i,j) \in \mathcal{E}$.

However, feasibility of bearing constraints does not imply uniqueness of the target formation. A target formation is unique up to a translation and scaling factor if the bearing constraints $\{g^\star_{ij}\}_{(i,j)\in\mathcal{E}}$ specify an infinitesimal bearing rigid framework. For the nonlinear bearing-only control law proposed in (D.1), the following results hold,

i) The centroid and scale of the formation are invariant,

ii) If the target formation is infinitesimally bearing rigid, then the system has two isolated equilibria and the system is almost globally exponentially stable.

A simulation result for the system in (D.1) and graph D.5 is shown in Figure D.4 where Figure D.4a shows the desired stationary formation and Figure D.4b shows the bearing error where se see that $g_{ij}(t)$ equals $g^\star_{ij}$ asymptotically.

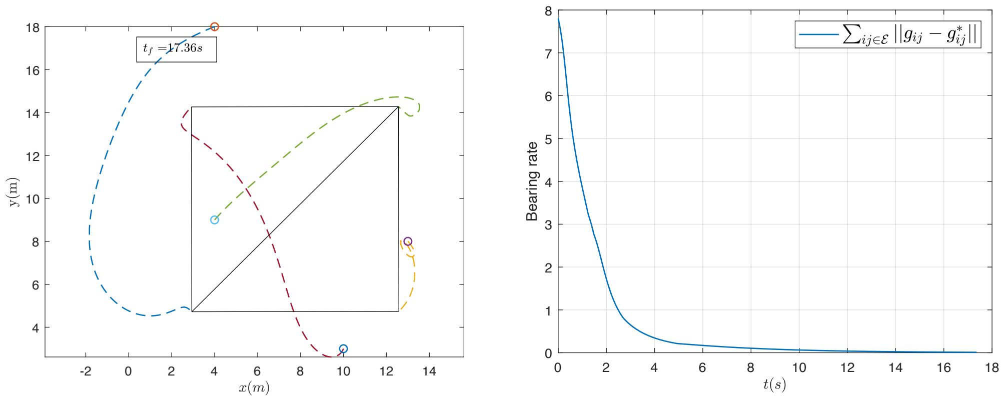

(a) Formation trajectory of the system (D.1).

(b) Evolution of bearing error $\sum_{(i,j)\in\mathcal{E}} \|g_{ij} - g^\star_{ij}\|$.

Figure D.4: Simulation of the system in (D.1).

This section is built on the assumption that agent model is of single integrator dynamics. Next we present some results from [14] where agents are modeled with double integrator dynamics which is also the case in Chapter 4. For agents modeled as $\dot{p}_i(t) = v_i(t), \dot{v}_i(t) = u_i(t)$ where $u_i(t)$ is the acceleration input, the proposed bearing-only control law is,

$$\begin{aligned} \dot{p}_i(t) &= v_i(t), \\ \dot{v}_i(t) &= k_p \sum_{j\in\mathcal{N}_i} (g_{ij}(t) - g^\star_{ij}) + k_v \sum_{j\in\mathcal{N}_i} \dot{g}_{ij}(t), \end{aligned} \tag{D.2}$$

where k_p and k_v are position and velocity gains respectively. Using the above control law, $g_{ij}(t)$ converges to $g^\star_{ij}$ and $\dot{g}_{ij}(t)$ converges to 0. To see the working of system in

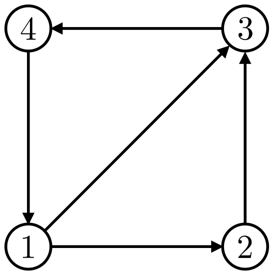

Figure D.5: An undirected graph

(D.2), consider the graph in D.5 where each agent's control is,

$$
\begin{aligned}
u_1(t) &= k_p(g_{12} - g_{12}^\star + g_{13} - g_{13}^\star + g_{14} - g_{14}^\star) + k_v(\dot{g}_{12} + \dot{g}_{13} + \dot{g}_{14}),\\
u_2(t) &= k_p(g_{21} - g_{21}^\star + g_{23} - g_{23}^\star) + k_v(\dot{g}_{21} + \dot{g}_{23}),\\
u_3(t) &= k_p(g_{31} - g_{31}^\star + g_{32} - g_{32}^\star + g_{34} - g_{34}^\star) + k_v(\dot{g}_{31} + \dot{g}_{32} + \dot{g}_{34}),\\
u_4(t) &= k_p(g_{41} - g_{41}^\star + g_{43} - g_{43}^\star) + k_v(\dot{g}_{41} + \dot{g}_{43}),
\end{aligned}
$$

and the Figure D.6 shows the corresponding simulation results. We see that formation is achieved in Figure D.6a and the bearing error $\sum_{j\in\mathcal{N}_i} \|g_{ij} - g_{ij}^\star\|$ and rate of bearing vectors $\sum_{j\in\mathcal{N}_i}$ are shown in Figure D.6b and D.6c respectively.

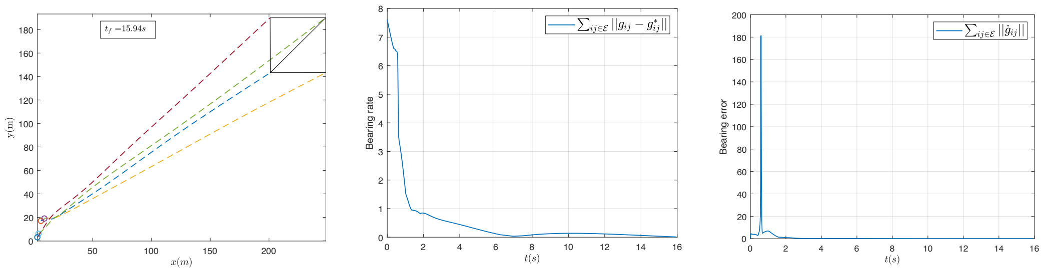

(a) Formation trajectory for the control law (D.2).

(b) Evolution of bearing error $\sum_{(i,j)\in\mathcal{E}} \|g_{ij} - g_{ij}^\star\|$.

(c) Evolution of bearing rate $\sum_{(i,j)\in\mathcal{E}} \|\dot{g}_{ij}\|$.

Figure D.6: Simulation of the system in (D.2).

As stated earlier, the controller (D.2) drives the bearing vectors $g_{ij}(t)$ to $g_{ij}^\star$ and rate of bearings $\dot{g}_{ij}(t)$ to 0.

Bibliography

[1] R. Olfati-Saber, J. A. Fax, and R. M. Murray, "Consensus and cooperation in networked multi-agent systems," *Proceedings of the IEEE*, vol. 95, no. 1, pp. 215–233, 2007.

[2] M. Mesbahi and M. Egerstedt, *Graph theoretic methods in multiagent networks*, vol. 33. Princeton University Press, 2010.

[3] Y. Shoham and K. Leyton-Brown, *Multiagent systems: Algorithmic, game-theoretic, and logical foundations.* Cambridge University Press, 2008.

[4] Y. Wang, E. Garcia, D. Casbeer, and F. Zhang, *Cooperative control of multi-agent systems: Theory and applications.* John Wiley & Sons, 2017.

[5] W. Ren, R. W. Beard, and E. M. Atkins, "A survey of consensus problems in multi-agent coordination," in *Proceedings of the 2005, American Control Conference, 2005.*, pp. 1859–1864, IEEE, 2005.

[6] J. N. Tsitsiklis, "Problems in decentralized decision making and computation.," tech. rep., Massachusetts Inst of Tech Cambridge Lab for Information and Decision Systems, 1984.

[7] V. Borkar and P. Varaiya, "Asymptotic agreement in distributed estimation," *IEEE Transactions on Automatic Control*, vol. 27, no. 3, pp. 650–655, 1982.

[8] B. Briegel, D. Zelazo, M. Bürger, and F. Allgöwer, "On the zeros of consensus networks," in *2011 50th IEEE Conference on Decision and Control and European Control Conference*, pp. 1890–1895, IEEE, 2011.

[9] F. Bullo, *Lectures on Network Systems.* 1 ed., 2019.

[10] H.-S. Ahn, *Formation Control Approaches for Distributed Agents.* Studies in Systems, Decision and Control, 205, Cham: Springer International Publishing, 1st ed. 2020. ed.

[11] K.-K. Oh, M.-C. Park, and H.-S. Ahn, "A survey of multi-agent formation control," *Automatica*, vol. 53, pp. 424–440, 2015.

[12] S. Zhao and D. Zelazo, "Bearing rigidity and almost global bearing-only formation stabilization," *IEEE Transactions on Automatic Control*, vol. 61, no. 5, pp. 1255–1268, 2016.

[13] S. Zhao and D. Zelazo, "Translational and scaling formation maneuver control via a bearing-based approach," *IEEE Transactions on Control of Network Systems*, vol. 4, no. 3, pp. 429–438, 2015.

[14] S. Zhao, Z. Li, and Z. Ding, "Bearing-only formation tracking control of multi-agent systems," *IEEE Transactions on Automatic Control*, 2019.

[15] D. V. Dimarogonas, E. Frazzoli, and K. H. Johansson, "Distributed event-triggered control for multi-agent systems," *IEEE Transactions on Automatic Control*, vol. 57, no. 5, pp. 1291–1297, 2012.

[16] C. Nowzari, E. Garcia, and J. Cortés, "Event-triggered communication and control of networked systems for multi-agent consensus," *Automatica*, vol. 105, pp. 1–27, 2019.

[17] W. Heemels, K. H. Johansson, and P. Tabuada, "An introduction to event-triggered and self-triggered control," in *2012 IEEE 51st IEEE Conference on Decision and Control (CDC)*, pp. 3270–3285, IEEE, 2012.

[18] M. Sewlia and D. Zelazo, "Distributed event-based control for second-order multi-agent systems," in *2019 27th Mediterranean Conference on Control and Automation (MED)*, pp. 310–315, IEEE, 2019.

[19] C. Nowzari, E. Garcia, and J. Cortés, "Event-triggered communication and control of networked systems for multi-agent consensus," *Automatica*, vol. 105, pp. 1–27, 2019.

[20] P. J. Gawthrop and L. Wang, "Event-driven intermittent control," *International Journal of Control*, vol. 82, no. 12, pp. 2235–2248, 2009.

[21] W. Wasylkiwskyj, *Signals and transforms in linear systems analysis.* Springer, 2013.

[22] L. Guzzella, "Discrete-time control systems," *ETH Zurich*, 2009.

[23] G. S. Seyboth, D. V. Dimarogonas, and K. H. Johansson, "Event-based broadcasting for multi-agent average consensus," *Automatica*, vol. 49, no. 1, pp. 245–252, 2013.

[24] X. Meng and T. Chen, "Event based agreement protocols for multi-agent networks," *Automatica*, vol. 49, no. 7, pp. 2125–2132, 2013.

[25] H. Li, X. Liao, G. Chen, D. J. Hill, Z. Dong, and T. Huang, "Event-triggered asynchronous intermittent communication strategy for synchronization in complex dynamical networks," *Neural Networks*, vol. 66, pp. 1–10, 2015.

[26] G. S. Seyboth, D. V. Dimarogonas, and K. H. Johansson, "Control of multi-agent systems via event-based communication," *IFAC Proceedings Volumes*, vol. 44, no. 1, pp. 10086–10091, 2011.

[27] D. Xue and S. Hirche, "Event-triggered consensus of heterogeneous multi-agent systems with double-integrator dynamics," in *2013 European Control Conference (ECC)*, pp. 1162–1167, IEEE, 2013.

[28] E. Garcia, Y. Cao, and D. W. Casbeer, "Decentralised event-triggered consensus of double integrator multi-agent systems with packet losses and communication delays," *IET Control Theory & Applications*, vol. 10, no. 15, pp. 1835–1843, 2016.

[29] X. Yi, J. Wei, D. V. Dimarogonas, and K. H. Johansson, "Formation control for multi-agent systems with connectivity preservation and event-triggered controllers," *IFAC-PapersOnLine*, vol. 50, no. 1, pp. 9367–9373, 2017.

[30] M.-Z. Dai and F. Xiao, "Event-and self-triggered consensus for double-integrator networks with relative state measurements," *International Journal of Control*, vol. 93, no. 5, pp. 1194–1203, 2020.

[31] Q. Liu *et al.*, "Event-triggered consensus and formation control in multi-agent coordination," 2018.

[32] Y. Yu, Z. Zeng, Z. Li, X. Wang, and L. Shen, "Event-triggered encirclement control of multi-agent systems with bearing rigidity," *Science China Information Sciences*, vol. 60, no. 11, p. 110203, 2017.

[33] X. Ge and Q.-L. Han, "Distributed formation control of networked multi-agent systems using a dynamic event-triggered communication mechanism," *IEEE Transactions on Industrial Electronics*, vol. 64, no. 10, pp. 8118–8127, 2017.

[34] L. Zhang, X. Li, J. Yan, and X. Guan, "Event-triggered multitarget formation control for multiagent systems," *Mathematical Problems in Engineering*, vol. 2017, 2017.

[35] Z. Sun, Q. Liu, C. Yu, and B. D. Anderson, "Generalized controllers for rigid formation stabilization with application to event-based controller design," in *2015 European Control Conference (ECC)*, pp. 217–222, IEEE, 2015.

[36] K.-E. Åarzén, "A simple event-based pid controller," *IFAC Proceedings Volumes*, vol. 32, no. 2, pp. 8687–8692, 1999.

[37] M. Velasco, J. Fuertes, and P. Marti, "The self triggered task model for real-time control systems," in *Work-in-Progress Session of the 24th IEEE Real-Time Systems Symposium (RTSS03)*, vol. 384, 2003.

[38] M. Mazo Jr, A. Anta, and P. Tabuada, "An iss self-triggered implementation of linear controllers," *Automatica*, vol. 46, no. 8, pp. 1310–1314, 2010.

[39] C. Nowzari and J. Cortés, "Team-triggered coordination of networked systems," in *2013 American Control Conference*, pp. 3821–3826, IEEE, 2013.

[40] P. Tabuada, "Event-triggered real-time scheduling of stabilizing control tasks," *IEEE Transactions on Automatic Control*, vol. 52, no. 9, pp. 1680–1685, 2007.

[41] H. K. Khalil and J. Grizzle, *Nonlinear systems*, vol. 3. Prentice hall Upper Saddle River, NJ, 2002.

[42] K. J. Astrom and B. M. Bernhardsson, "Comparison of riemann and lebesgue sampling for first order stochastic systems," in *Proceedings of the 41st IEEE Conference on Decision and Control, 2002.*, vol. 2, pp. 2011–2016, IEEE, 2002.

[43] B. A. Khashooei, D. J. Antunes, and W. Heemels, "Output-based event-triggered control with performance guarantees," *IEEE Transactions on Automatic Control*, vol. 62, no. 7, pp. 3646–3652, 2017.

[44] L. Mi and L. Mirkin, "h_∞ event-triggered control with performance guarantees vis-à-vis optimal periodic control," in *2019 IEEE 58th Conference on Decision and Control (CDC)*, pp. 187–192, IEEE, 2019.

[45] D. P. Borgers, V. Dolk, and W. Heemels, "Dynamic event-triggered control with time regularization for linear systems," in *2016 IEEE 55th Conference on Decision and Control (CDC)*, pp. 1352–1357, IEEE, 2016.

[46] A. Girard, "Dynamic triggering mechanisms for event-triggered control," *IEEE Transactions on Automatic Control*, vol. 60, no. 7, pp. 1992–1997, 2014.

[47] A. Selivanov and E. Fridman, "Event-triggered h_∞ control: A switching approach," *IEEE Transactions on Automatic Control*, vol. 61, no. 10, pp. 3221–3226, 2015.

[48] A. D. Ames, P. Tabuada, and S. Sastry, "On the stability of zeno equilibria," in *International Workshop on Hybrid Systems: Computation and Control*, pp. 34–48, Springer, 2006.

[49] M. Heymann, F. Lin, G. Meyer, and S. Resmerita, "Analysis of zeno behaviors in a class of hybrid systems," *IEEE Transactions on Automatic Control*, vol. 50, no. 3, pp. 376–383, 2005.

[50] N. Huggett, "Zeno's paradoxes," in *The Stanford Encyclopedia of Philosophy* (E. N. Zalta, ed.), Metaphysics Research Lab, Stanford University, winter 2019 ed., 2019.

[51] W. H. Heemels, M. Donkers, and A. R. Teel, "Periodic event-triggered control for linear systems," *IEEE Transactions on Automatic Control*, vol. 58, no. 4, pp. 847–861, 2012.

[52] W. Ren and R. W. Beard, *Distributed consensus in multi-vehicle cooperative control.* Springer, 2008.

[53] W. Ren and E. Atkins, "Second-order consensus protocols in multiple vehicle systems with local interactions," in *AIAA Guidance, Navigation, and Control Conference and Exhibit*, p. 6238, 2005.

[54] G. H. Hardy, J. E. Littlewood, G. Pólya, *et al.*, *Inequalities.* Cambridge university press, 1988.

[55] D. P. Borgers and W. Heemels, "On minimum inter-event times in event-triggered control," in *52nd IEEE Conference on Decision and Control*, pp. 7370–7375, IEEE, 2013.

[56] T. Hu, Z. Lin, and Y. Shamash, "On maximizing the convergence rate for linear systems with input saturation," *IEEE Transactions on Automatic Control*, vol. 48, no. 7, pp. 1249–1253, 2003.

[57] P. Tabuada, "Event-triggered real-time scheduling of stabilizing control tasks," *IEEE Transactions on Automatic Control*, vol. 52, no. 9, pp. 1680–1685, 2007.

[58] D. Tolić and S. Hirche, *Networked control systems with intermittent feedback.* Crc Press, 2017.

[59] C. Godsil and G. F. Royle, *Algebraic graph theory*, vol. 207. Springer Science & Business Media, 2013.

בקרה מבוזרת מבוססת אירועים של מערכות מרובות סוכנים בעלי דינמיקה מסדר שני

מאיאנק סווליה

בקרה מבוזרת מבוססת אירועים של מערכות מרובות סוכנים בעלי דינמיקה מסדר שני

חיבור על מחקר

לשם מילוי חלקי של הדרישות לקבלת
מגיסטר למדעים בהנדסת אוירונוטיקה וחלל

מאיאנק סווליה

הוגש לסנט נטכניון – מכון טכנולוגי לישראל

סיון תש"ף　　חיפה　　יוני 2020

(עמוד זה הושאר ריק במכוון)

המחקר בוצע בהנחייתו של פרופסור דניאל זלזו בפקולטה להנדסת אוירונאוטיקה וחלל